

OPEN

# Mechanisms of GABA<sub>B</sub> receptor enhancement of extrasynaptic GABA<sub>A</sub> receptor currents in cerebellar granule cells

Shailesh N. Khatri<sup>1</sup>, Wan-Chen Wu<sup>1</sup>, Ying Yang<sup>1,2</sup> & Jason R. Pugh<sup>1,3\*</sup>

Many neurons, including cerebellar granule cells, exhibit a tonic GABA current mediated by extrasynaptic GABA<sub>A</sub> receptors. This current is a critical regulator of firing and the target of many clinically relevant compounds. Using a combination of patch clamp electrophysiology and photolytic uncaging of RuBi-GABA we show that GABA<sub>B</sub> receptors are tonically active and enhance extrasynaptic GABA<sub>A</sub> receptor currents in cerebellar granule cells. This enhancement is not associated with meaningful changes in GABA<sub>A</sub> receptor potency, mean channel open-time, open probability, or single-channel current. However, there was a significant (~40%) decrease in the number of channels participating in the GABA uncaging current and an increase in receptor desensitization. Furthermore, we find that adenylylase, PKA, CaMKII, and release of Ca<sup>2+</sup> from intracellular stores are necessary for modulation of GABA<sub>A</sub> receptors. Overall, this work reveals crosstalk between postsynaptic GABA<sub>A</sub> and GABA<sub>B</sub> receptors and identifies the signaling pathways and mechanisms involved.

The  $\gamma$ -amino butyric acid A receptors (GABA<sub>A</sub>Rs) are major contributors of cellular inhibition in the central nervous system. These receptors can be broadly divided into two classes based on composition and location, synaptic and extrasynaptic receptors. GABA<sub>A</sub>Rs are pentameric ligand gated ion channels, generally consisting of two  $\alpha$ -subunits, two  $\beta$ -subunits, and either a  $\gamma$ - or  $\delta$ -subunit. GABA<sub>A</sub>Rs containing a  $\gamma$ -subunit are targeted to the synaptic space where they are activated by synaptically released GABA and mediate phasic inhibition<sup>1,2</sup>. GABA<sub>A</sub>Rs containing a  $\delta$ -subunit ( $\delta$ -GABA<sub>A</sub>Rs), on the other hand, are found primarily in the extrasynaptic space where they experience limited exposure to synaptic GABA release and play little<sup>3</sup> or no role in phasic inhibition<sup>4</sup>. However,  $\delta$ -GABA<sub>A</sub>Rs show a higher affinity for GABA and can be tonically activated by ambient GABA in the extracellular space<sup>5</sup>. This produces a small but powerful tonic inhibitory current in cells expressing  $\delta$ -subunit containing receptors, capable of dramatically influencing firing<sup>6,7</sup>. This has made extrasynaptic  $\delta$ -GABA<sub>A</sub>Rs an important target for modulation. For example, the drug 4,5,6,7-Tetrahydroisothiazolo-[5,4-c]pyridine-3-ol (THIP or gaboxadol)<sup>8</sup>, the anesthetic propofol<sup>9</sup>, and ethanol<sup>10–13</sup>, preferentially activate  $\delta$ -GABA<sub>A</sub>Rs. Likewise, modulation of  $\delta$ -GABA<sub>A</sub>Rs by endogenous neurosteroids contributes to responses to stress and postpartum depression<sup>14–16</sup>.

Recent studies have shown that activation of GABA<sub>B</sub> receptors (GABA<sub>B</sub>Rs) can also modulate extrasynaptic  $\delta$ -GABA<sub>A</sub>Rs. Application of GABA<sub>B</sub>R agonists increases tonic GABA<sub>A</sub>R currents in cerebellar granule cells, dentate granule cells, and thalamic relay neurons, while GABA<sub>B</sub>R antagonists decrease the tonic current<sup>17,18</sup>. Furthermore, our studies suggest that presynaptic GABA<sub>A</sub>Rs may also be enhanced by activation of GABA<sub>B</sub>Rs in parallel fiber presynaptic terminals<sup>19,20</sup>. These findings open new opportunities to indirectly target tonic GABA currents mediated by  $\delta$ -GABA<sub>A</sub>Rs. However, the signaling mechanisms linking GABA<sub>B</sub>R activity to  $\delta$ -GABA<sub>A</sub>Rs and the biophysical mechanisms of GABA<sub>A</sub>R enhancement are not currently understood.

To address these questions, we made whole-cell patch-clamp recordings from granule cells in acute cerebellar slices, and GABA<sub>A</sub>R currents were evoked by photolytic release of GABA from RuBi-GABA. We found that blocking GABA<sub>B</sub>Rs by bath application of CGP55845 or 2hydroxy-saclofen reduced GABA<sub>A</sub>R currents to

<sup>1</sup>University of Texas Health Science Center at San Antonio, Department of Cellular and Integrative Physiology, San Antonio, TX, 78229, USA. <sup>2</sup>Xiangya School of Medicine, Central South University, Changsha, Hunan, China. <sup>3</sup>Center for Biomedical Neuroscience, University of Texas Health Science Center at San Antonio, San Antonio, Texas, 78229, USA. \*email: [pughj@uthscsa.edu](mailto:pughj@uthscsa.edu)

~60% of control, suggesting GABA<sub>A</sub>R currents are constitutively enhanced by GABA<sub>B</sub>Rs. GABA<sub>B</sub>R antagonists had no effect on GABA<sub>A</sub>R currents in Purkinje or stellate cells, or on GABA<sub>A</sub>R currents evoked by synaptic GABA release in granule cells. Non-stationary fluctuation analysis suggests the change in GABA<sub>A</sub>R current results from a reduction in number of GABA<sub>A</sub>Rs activated, at least partially due to increased desensitization. Enhancement of GABA<sub>A</sub>R currents by GABA<sub>B</sub>Rs requires G-protein signaling, adenylate cyclase, PKA, and Ca<sup>2+</sup>/calmodulin-dependent protein kinase II (CaMKII). The reduction in GABA<sub>A</sub>R current by GABA<sub>B</sub>R antagonists was mimicked and occluded by high intracellular EGTA, suggesting changes in intracellular calcium are necessary. Inhibition of ryanodine receptors, but not L-type calcium channels, blocked the effects of GABA<sub>B</sub>R antagonists, suggesting GABA<sub>B</sub>R modulation works through release of calcium from intracellular stores.

## Results

**Extrasynaptic GABA<sub>A</sub>Rs are modulated by tonically active GABA<sub>B</sub>Rs.** In order to investigate the mechanisms by which GABA<sub>B</sub>Rs enhance GABA<sub>A</sub>R-mediated currents we made whole-cell patch clamp recordings from granule cells in acute cerebellar slices. GABA currents were evoked by full field uncaging of RuBi-GABA (60 μM) using a brief (5 ms) light pulse from a 470 nm LED or 473 nm laser (Fig. 1A). The resultant current is referred to as the “uncaging current”. Uncaging currents were completely blocked by application of picrotoxin (100 μM), indicating these currents are mediated by GABA<sub>A</sub>Rs (Fig. 1B, top). G-protein coupled inward rectifying K<sup>+</sup> (GIRK) currents potentially linked to GABA<sub>B</sub>R activity are likely inhibited in our experiments by CsCl and QX-314 in the internal solution<sup>21,22</sup>. Despite the lack of GABA<sub>B</sub>R-mediated currents, bath application of the GABA<sub>B</sub>R antagonists CGP55845 (CGP, 3 μM) or saclofen (200 μM) reduced the amplitude of the uncaging current (CGP: 58.8 ± 2.7% of control, n = 9, p < 0.001; saclofen: 65.6 ± 5.7% of control, n = 6, p = 0.004; Fig. 1B), suggesting GABA<sub>A</sub>Rs are constitutively enhanced by GABA<sub>B</sub>R activity. Application of CGP or saclofen also reduced the 10–90 rise-time (24.9 ± 5.1 vs. 17.6 ± 3.1 ms, n = 15, p = 0.02) and decay-time constant (719.3 ± 101.3 vs. 497.0 ± 68.0 ms, p = 0.003) of the uncaging current (Fig. 1B,C). In the absence of CGP application, uncaging current amplitudes in granule cells were stable over 15 minutes of repeated uncaging (last response: 95.8 ± 2.7% of first response, n = 7, p = 0.18; Fig. 1D), suggesting the decrease in uncaging current amplitude is not due to rundown of the response or accumulation of GABA in the slice or bath solution. In Purkinje or stellate cells of the cerebellum, application of CGP had no effect on GABA uncaging current amplitudes (Purkinje: 103.4 ± 9.9% of control, n = 6, p = 0.83; stellate: 101.2 ± 4.6% of control, n = 7, p = 0.67; Fig. 1E,F), indicating enhancement of GABA<sub>A</sub>Rs is specific to granule cells. Furthermore, synaptic IPSCs evoked by electrical stimulation in granule cells were not affected by application of CGP (119.9 ± 14.7% of control, n = 8, p = 0.21; Fig. 1G), suggesting that modulation by GABA<sub>B</sub>Rs is specific to extrasynaptic GABA<sub>A</sub>Rs. This profile of activity matches δ-subunit containing GABA<sub>A</sub>Rs expressed in cerebellar granule cells which mediate tonic inhibition<sup>23</sup>. This suggests GABA<sub>B</sub>R modulation is specific to δ-GABA<sub>A</sub>Rs, as has been found previously<sup>17,18</sup>. However, our GABA uncaging protocol may activate both synaptic and extrasynaptic GABA<sub>A</sub>Rs, in order to demonstrate the same effect of CGP on isolated currents from extrasynaptic receptors, we recorded tonic GABA<sub>A</sub>R currents by measuring the change in the holding current following application of bicuculline (20 μM), a GABA<sub>A</sub>R antagonist. In the presence of CGP the tonic GABA<sub>A</sub>R current was decreased to 42.4% of control (n = 7, p < 0.05 unpaired t-test, Fig. 1H) similar to the reduction of uncaging currents in the presence of CGP. We therefore used GABA uncaging in further experiments to investigate the signaling mechanisms involved in extrasynaptic GABA<sub>A</sub>R modulation.

The observation that application of a GABA<sub>B</sub>R antagonist alone is sufficient to reduce the uncaging current suggests that at least a fraction of GABA<sub>B</sub>Rs are tonically activated in our experiments. This is consistent with a previous study which found that ambient GABA tonically activates GABA<sub>B</sub>Rs on Golgi cell terminals in the granule cell layer<sup>24</sup>. Furthermore, application of 100 μM baclofen, a GABA<sub>B</sub>R agonist, did not increase the uncaging GABA current amplitude (94.8 ± 6.2% of control, n = 6, p = 0.48; Fig. 2A), consistent with constitutive activation of GABA<sub>B</sub>Rs. In these experiments, GABA<sub>B</sub>Rs could be activated by endogenous ambient GABA in the granule cell layer<sup>6</sup> or build-up of GABA in the slice due to repeated uncaging. In order to test for the presence of constitutive activation of GABA<sub>B</sub>Rs in the absence of repeated GABA uncaging, we activated GABA<sub>A</sub>Rs by local pressure application of 10 μM muscimol (a GABA<sub>A</sub>R specific agonist highly selective for δ-subunit GABA<sub>A</sub>Rs and tonic currents at low concentrations<sup>25,26</sup>) onto granule cells. Under these conditions we found that CGP still reduced the GABA<sub>A</sub>R current (67.0 ± 4.2% of control, n = 8, p = 0.002; Fig. 2B), similar to results from GABA uncaging. This suggests that GABA<sub>B</sub>Rs in granules cells are tonically activated by endogenous ambient GABA, not buildup of uncaged GABA in the bath solution.

In addition to granule cells, GABA<sub>B</sub>Rs are also expressed on the soma and axon terminals of GABAergic Golgi cells within the granule cell layer<sup>24,27</sup>, raising the possibility that the effects of CGP on GABA<sub>A</sub>R currents is mediated by network effects in the granule cell layer. A previous study found that GABA<sub>B</sub>Rs in Golgi cell terminals inhibit GABA release<sup>24</sup>, suggesting that blocking these receptors could increase GABA release in the granule cell layer. Moreover, in cell attached recordings we found that application of CGP increased the spontaneous firing rate of Golgi cells (226.4 ± 39.81% of control, p = 0.02, n = 3), which is also expected to increase GABA release. This raises the possibility that CGP acts on GABA<sub>A</sub>Rs through increasing the ambient extracellular GABA concentration in the granule cell layer. This could reduce the uncaging GABA current through either increasing desensitization of GABA<sub>A</sub>Rs<sup>5</sup> or increasing the fraction of receptors tonically activated (and reducing the fraction of receptors available to be activated by GABA uncaging). We tested this possibility by applying 10 μM NNC-711, a GABA transporter blocker, to raise the ambient GABA level. In four out of four cells NNC-711 increased the tonic GABA current (data not shown), confirming an increase in ambient GABA. NNC-711 reduced the uncaging current amplitude (71.4 ± 4.4% of control, n = 7, p = 0.007), but subsequent application of CGP was still able to reduce the uncaging current amplitude further (72.2 ± 4.4% of NNC-711, n = 7, p = 0.002, Fig. 2C). These data indicate that increasing the ambient GABA level can alter GABA uncaging currents, but this does not occlude the reduction in uncaging current amplitude by CGP. In a second set of experiment, GDP-β-S was included in the internal solution to inhibit G-protein coupled signaling in the patched cell. In this case, CGP had little effect



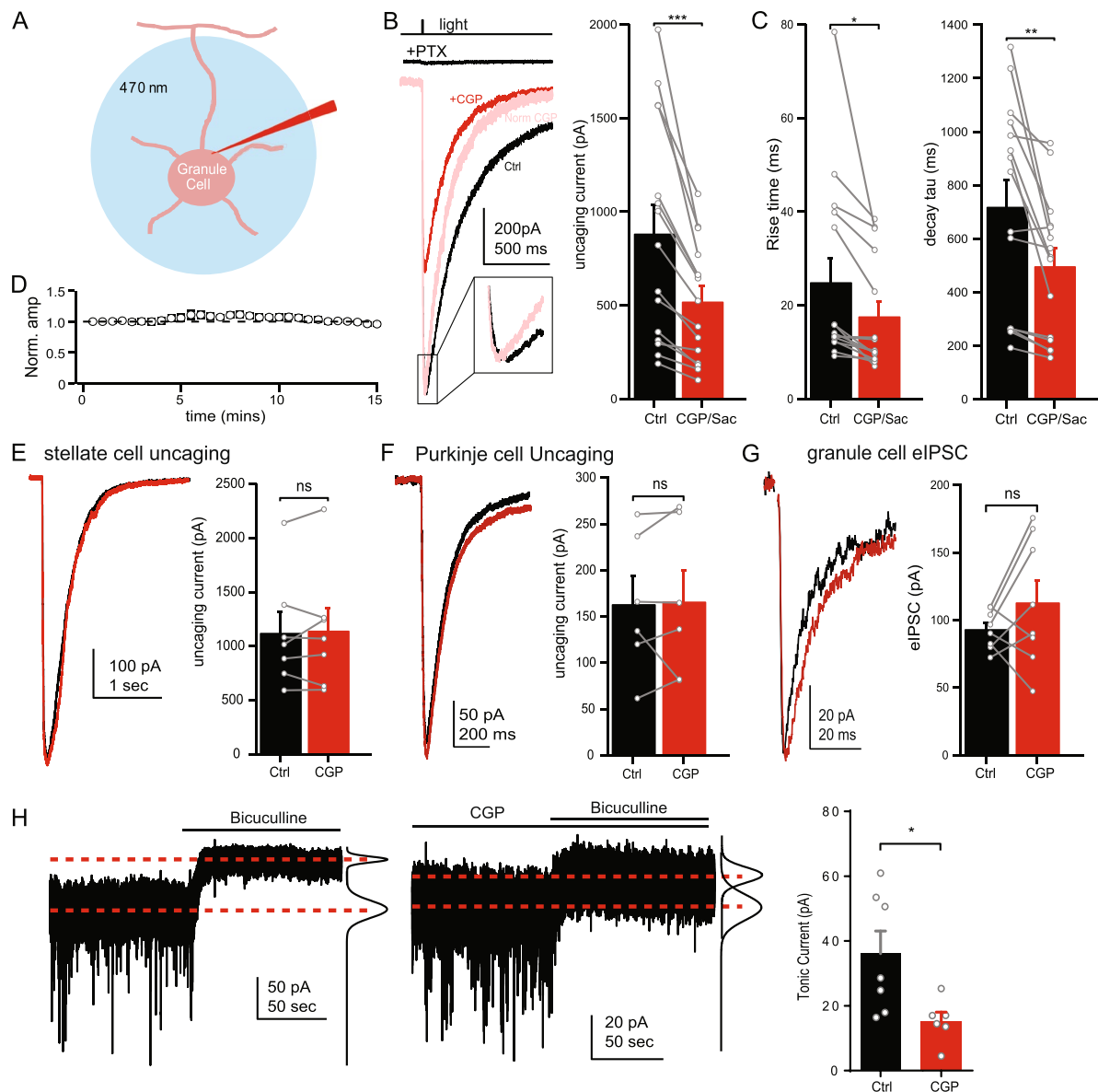


**Figure 1.** GABA<sub>B</sub>Rs enhance extrasynaptic GABA<sub>A</sub>Rs. (A) Schematic view of experimental design including whole-cell patch clamp recording from granule cells and uncaging of RuBi-GABA by 470 nm LED/Laser light pulse. (B) Left: Diagram of GABA uncaging light pulse (top) and resulting currents recorded in a granule cell in the presence of picrotoxin (+PTX), standard ACSF (black), or CGP55845 (red). The CGP trace normalized to the peak of the control trace is also displayed (pink) to show the change in decay kinetics and rise time (inset). Right: Average amplitudes of uncaging current in control (black) and in the presence of CGP55845 or saclofen (red). (C) Average rise time (left) and decay time constant (right) of GABA uncaging currents in control ACSF (black) or in the presence of CGP55845 or saclofen (red). (D) Average uncaging current amplitudes over 15 minutes in control ACSF. (E,F) Example traces (left) and average amplitudes (right) of uncaging currents in control ACSF (black) and in the presence of CGP55845 (red) in stellate cells (E) and Purkinje cells (F). (G) Example traces (left) and average amplitudes (right) of evoked inhibitory postsynaptic currents in control ACSF (black) and in the presence of CGP55845 (red) in granule cells. (H) Example traces of tonic GABA<sub>A</sub> receptor currents in control ACSF (left) and in the presence of CGP (middle). Average holding current values (dashed red line) and Gaussian fits of histograms of current values (black lines) before and after bicucullin application are also shown. Right: Average tonic GABA<sub>A</sub> receptor currents in control ACSF (black) and in the presence of CGP (red). Data from individual cells are plotted as connected gray markers. (\*) indicates  $p$ -value  $\leq 0.05$ , (\*\*) indicates  $p$ -value  $\leq 0.01$ , (\*\*\*) indicates  $p$ -value  $\leq 0.001$ , ns indicates  $p$ -value  $> 0.05$ .

on the uncaging current amplitude ( $92.8 \pm 3.3\%$  of control,  $n = 9$ ,  $p = 0.05$ ; Fig. 2D), suggesting that GABA<sub>B</sub>R signaling within the patched granule cell is necessary for enhancement of extrasynaptic GABA<sub>A</sub>Rs and ruling out network effects as a likely mechanism. This finding also confirms that CGP acts through a G-protein coupled receptors (GPCR) rather than binding to or altering GABA<sub>A</sub>Rs directly.

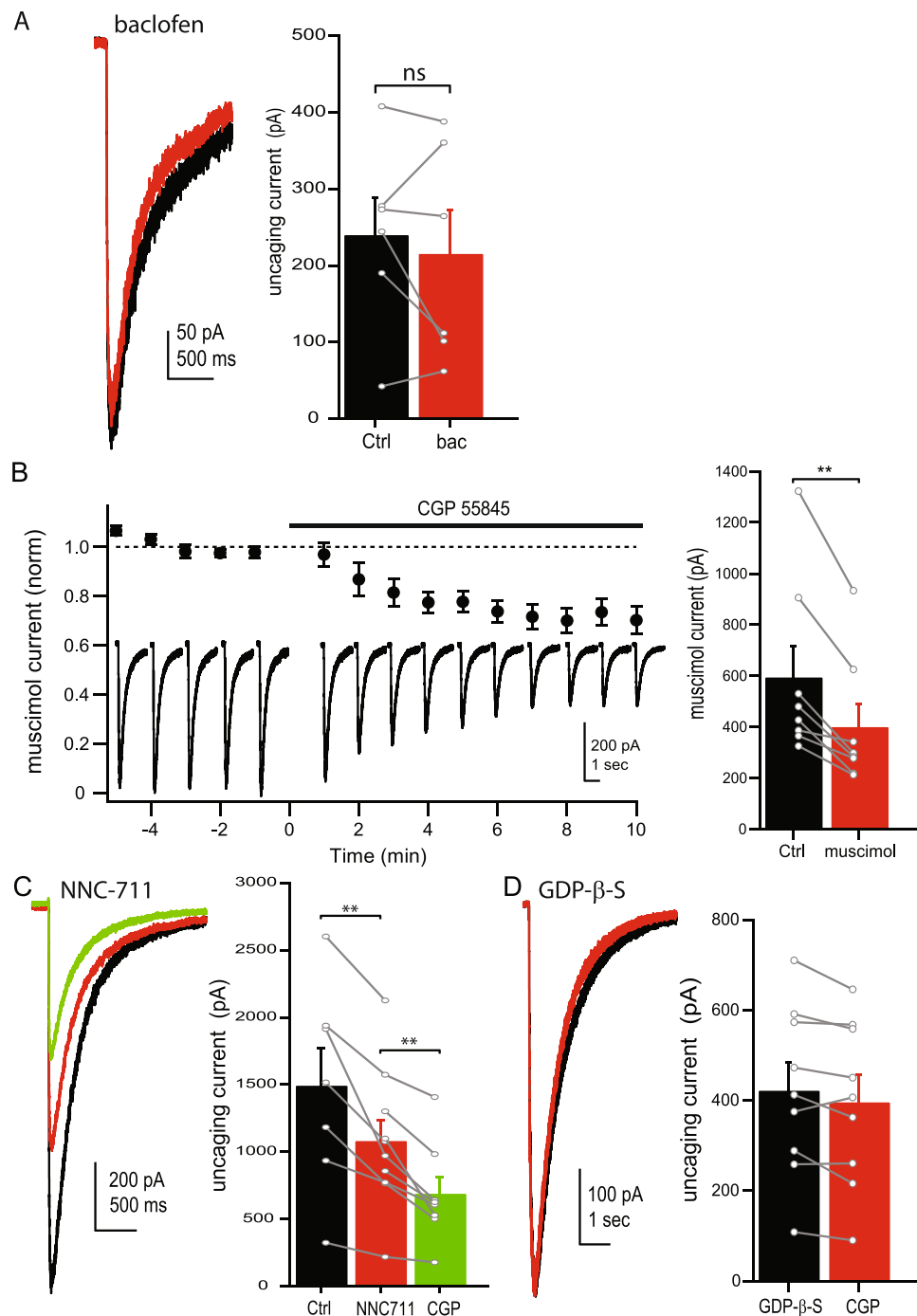


**Figure 2.** GABA<sub>B</sub>Rs are tonically active in granule cells. (A) Representative traces (left) and average amplitudes (right) of uncaging current in control ACSF (black) and in the presence of baclofen (red). (B) left: Average current amplitudes (circles) and example traces (inset) following pressure application of muscimol throughout the time course of the experiment. CGP55845 was bath applied at time = 0. Right: Average muscimol current amplitudes in control ACSF (black) and in the presence of CGP55845 (red). (C) Representative traces (left) and average amplitudes (right) of uncaging currents in control ACSF (black), in the presence of NNC-711 (red), and in CGP55845 (green). (D) Representative traces (left) and average amplitudes (right) of uncaging currents in control ACSF (black) and in the presence of CGP55845 (red) when GDP-β-S is included in the internal solution. Data from individual cells are plotted as connected gray markers. (\*\*) indicates  $p$ -value  $\leq 0.01$ , ns indicates  $p$ -value  $> 0.05$ .

**GABA<sub>B</sub> receptors increase the number of available GABA<sub>A</sub> receptors.** While previous studies and our data show that GABA<sub>B</sub>Rs enhance extrasynaptic GABA<sub>A</sub>Rs<sup>17,18</sup>, the biophysical mechanisms of this enhancement have not been investigated. We tested several potential mechanisms that could alter GABA<sub>A</sub>R currents, including changes in GABA potency, desensitization, single channel open time, single channel current, open probability, and number of receptors available.

To test whether GABA<sub>B</sub>R activity alters the GABA potency of GABA<sub>A</sub>Rs in granule cells we used a range of blue laser intensities to uncage increasing concentrations of GABA and recorded the resulting currents (Fig. 3A). From this data, we created a dose-response curve of GABA<sub>A</sub>Rs in control solutions and in the presence of CGP. We found that the uncaging current was reduced to ~60% of control for each laser intensity tested, with no right or leftward shift in the curve (Fig. 3B). In fact, when the responses in CGP were scaled to the maximum response in control, the curves show significant overlap (Fig. 3B, open circles), suggesting GABA<sub>B</sub>R activity does not change the GABA potency of GABA<sub>A</sub>Rs.

We also measured the mean-open times of GABA<sub>A</sub>Rs using power spectra analysis of GABA currents during long (12 sec) pressure applications of GABA in control ACSF and in the presence of CGP (see methods; Fig. 3C, inset). From these data we constructed plots of spectral density versus frequency for each cell, which were fit with Lorentzian functions. From these fits we were able to estimate the mean channel open times for each cell. We found a small, but significant, reduction in the fast-open time in the presence of CGP ( $0.45 \pm 0.02$  ms vs  $0.33 \pm 0.03$  ms,  $n = 6$ ,  $p < 0.001$ ; Fig. 3D), and no change in the slower open times ( $p > 0.05$ ). Baclofen had no effect on the fast open time ( $0.56 \pm 0.12$  ms vs  $0.48 \pm 0.15$  ms,  $n = 5$ ,  $p = 0.66$ ). The faster open-time may contribute to the more rapid rise-time and decay time of the GABA current, but likely does not account for the relatively large (~40%) reduction in the macroscopic current.

We then used non-stationary fluctuation analysis<sup>28–30</sup> of currents evoked by uncaging GABA to discern whether CGP induced a change in the single-channel conductance, open probability, or number of available GABA<sub>A</sub>Rs. For each cell we measured the current amplitude and variance during the decay phase of the current, from which a plot of variance versus the mean amplitude of the current was constructed and fit with a binomial model (see methods). From these fits we estimated the single channel conductance, open probability, and number of channels participating in the current for each cell before and after application of CGP (Fig. 3E). Application of CGP did not change the single channel conductance ( $118.8 \pm 12.4\%$ ,  $n = 12$ ,  $p = 0.24$ ) or maximum open probability ( $P_{O_{max}}$ ;  $99.3 \pm 2.9\%$ ,  $n = 12$ ,  $p = 0.56$ ) of GABA<sub>A</sub>Rs, however, the number of channels participating in the current was reduced to  $61.8 \pm 5.9\%$  of control ( $n = 12$ ,  $p = 0.005$ ; Fig. 3F). This matches closely the reduction in the macroscopic uncaging current observed (~60% of control). The decrease in number of channels participating in the current could represent removal of GABA<sub>A</sub>Rs from the membrane or accumulation of receptors into long-lasting desensitized states<sup>31</sup>.

Previous investigations of desensitization of extrasynaptic/ $\delta$ -subunit containing GABA<sub>A</sub>R have produced conflicting results, with some studies showing little or no desensitization<sup>32,33</sup> and other showing moderate to profound desensitization<sup>2,5,34</sup>. To test for desensitization in our preparation and whether it is altered by GABA<sub>B</sub>R activity, we delivered a pair of uncaging light pulses (1 second interval) and measured the peak current amplitudes. The second peak (measured from the baseline prior to the first peak) was consistently smaller than the first peak, indicating desensitization of GABA<sub>A</sub>Rs following the first GABA application (peak2/peak1:  $0.80 \pm 0.01$ ,  $n = 5$ ,  $p = 0.004$ ; Fig. 3G). Bath application of CGP, in addition to reducing both peak current amplitudes ( $p = 0.007$ ), also significantly reduced the ratio of the second peak to the first (peak2/peak1:  $0.80 \pm 0.01$  versus  $0.73 \pm 0.01$ ,  $p = 0.005$ ; Fig. 3H), indicating greater desensitization. This suggests that increased desensitization contributes to the decreased GABA<sub>A</sub>R current and kinetics. However, these changes in desensitization are likely not sufficient to completely account for the large (~40%) decrease in the number of GABA<sub>A</sub>Rs participating in the GABA current following CGP application, suggesting changes in receptor trafficking and internalization are also involved.

We then tested whether a simple change in the rate of desensitization could account for the changes observed following CGP application using a computer model of GABA<sub>A</sub>R gating based on the kinetic scheme first described by Jones and Westbrook<sup>35</sup>. The transition rates in the model were first optimized to fit the relatively slow rise-time and decay kinetics of GABA<sub>A</sub>R currents evoked by GABA uncaging in cerebellar granule cells (Fig. 3I, Table 1). In the model receptors were activated by a 5 ms square pulse of 60  $\mu$ M GABA followed by an exponential decay to mimic the time course and relatively low concentrations of GABA likely to result from our uncaging protocol. In order to test the effects of increasing desensitization, we increased the transition rate to the doubly bound desensitized state 5-fold. We found that this change alone was sufficient to closely replicate the observed effects of CGP on GABA<sub>A</sub>R currents, including reduced peak current, reduced rise-time of the current, and reduced rate of decay (Fig. 3I, Table 1). Furthermore, both the experimental and model currents were well fit by single exponential curves. The faster current decay in the model is surprising given that previous modeling of GABA<sub>A</sub>Rs have found that increasing desensitization results in slower, bi-exponential current decay<sup>35,36</sup> due to reopening of desensitized receptors before unbinding GABA. This difference in our results appears to be due primarily to the relatively slow back rate from the doubly bound desensitized state in our model, and may reflect unique properties of the extrasynaptic ( $\delta$ -subunit containing) GABA<sub>A</sub>Rs modeled here as opposed to synaptic ( $\gamma$ -subunit containing) receptors. While this modelling data replicates the experimental data in many aspects, this does not necessarily mean that same process takes place in granule cells. However, this does provide theoretical evidence that it is possible for an increase in the rate of desensitization to produce faster macroscopic current kinetics.

**Signaling mechanisms of GABA<sub>A</sub> receptor enhancement.** The G<sub>i/o</sub> coupled GPCRs, like GABA<sub>B</sub>Rs, have been shown to inhibit adenylyl cyclase which produces cAMP, a common second messenger molecule<sup>37,38</sup>. To test whether inhibition of adenylyl cyclase is required for enhancement of GABA<sub>A</sub>Rs we measured uncaging currents in granule cells before and after application of forskolin (an adenylyl cyclase activator) or SQ-22536 (an adenylyl cyclase inhibitor). We found that forskolin (10  $\mu$ M), reduced the uncaging current amplitude ( $65.3 \pm 5.8\%$  of control,  $n = 11$ ,  $p < 0.001$ ; Fig. 4A). Furthermore, application of CGP in the presence of forskolin had no further effect on the amplitude of uncaging currents ( $89.9 \pm 4.9\%$  of control,  $n = 5$ ,  $p = 0.11$ ), indicating activation of adenylyl cyclase mimics and occludes the effect of CGP. This is consistent with previous observations and our model in which adenylyl cyclase activity is disinhibited by application of CGP<sup>17,39,40</sup>. In the presence of the adenylyl cyclase inhibitor, SQ-22536 (100  $\mu$ M), application of CGP had only a minimal effect

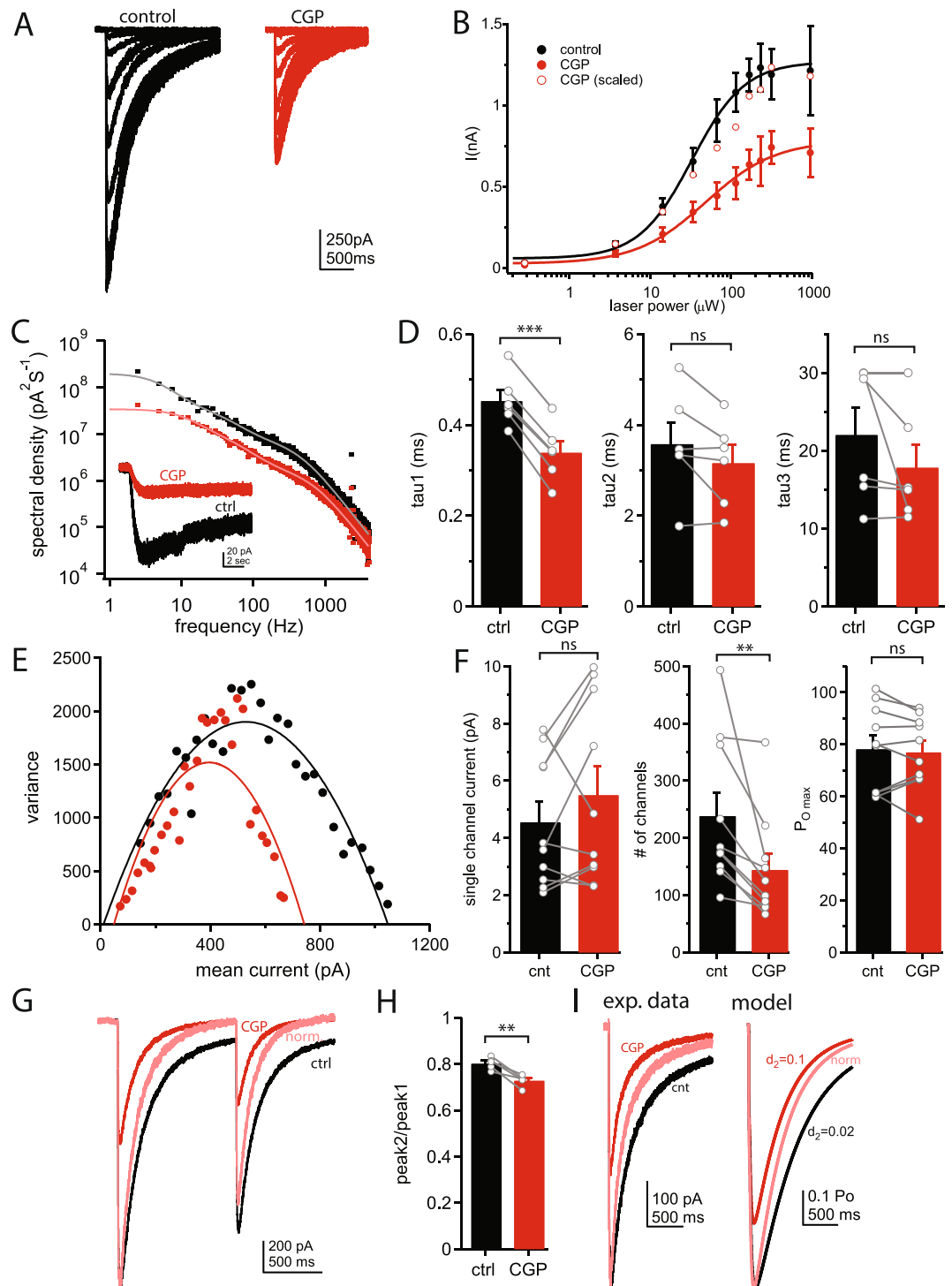


**Figure 3.** GABA<sub>B</sub> inhibition reduces the number of active GABA<sub>A</sub>Rs. **(A)** Representative traces of uncaging currents elicited by varying the uncaging laser intensity in control ACSF (left) and in the presence of CGP55845 (right). **(B)** Dose response curve showing the relationship between uncaging laser power and uncaging current amplitude in control ACSF (black) and in the presence of CGP55845 (red). Data are fit with Hill equation (lines). The CGP data normalized to the maximum current in control is also shown (open circles). **(C)** Example current traces (inset) and power spectral density plot of uncaging currents in control ACSF (black) and in the presence of CGP55845 (red). **(D)** Average values of fast (left) and slow (middle, right) time-constants determined by power spectral analysis in control ACSF (black) and in the presence of CGP55845 (red). **(E)** Example plot of non-stationary fluctuation analysis. Plot shows mean current amplitudes plotted against the variance of the current in control ACSF (black) and in the presence of CGP55845 (red) for a single cell. **(F)** Average single channel current (left), number of channels participating in the current (middle), and channel open probability ( $P_{O\max}$ ; right) in control ACSF (black) and in the presence of CGO55845 (red). **(G)** Representative uncaging current traces in control ACSF (black) on in the presence of CGP (red) following normalization. **(H)** Average ratio of peak2/peak1 in control ACSF (black) and in the presence of CGP (red). **(I)** Experimental data (left) and model fits (right) for control (black) and CGP (red) with  $d_2=0.1$  and  $d_2=0.02$ .



a pair of uncaging light pulses. The CGP trace normalized to the first peak of the control trace is also shown (pink) to demonstrate the change in paired-pulse ratio. **(H)** Average paired-pulse ratio in control ACSF (black) or in the presence of CGP55845 (red). **(I)** Left: Example traces of GABA uncaging currents in control ACSF (black) or in the presence of CGP (red). The CGP trace normalized to the peak of the control trace is also shown (pink) for comparison of kinetics. Right: Simulated GABA<sub>A</sub>R gating showing responses with relatively slow (black) and fast (red) desensitization. The fast desensitization trace normalized to the peak of the slow desensitization trace is also shown (pink) for comparison. *Control data (black) in (A) and (B) were previously published in Khatri et al.<sup>20</sup>. Data from individual cells are plotted as connected gray markers. (\*\*)* indicates  $p$ -value  $\leq 0.01$ , *(\*\*\*)* indicates  $p$ -value  $\leq 0.001$ , *ns* indicates  $p$ -value  $> 0.05$ .

on the uncaging current amplitude ( $89.1 \pm 5.2\%$  of control,  $n = 9$ ,  $p = 0.04$ ; Fig. 4B), suggesting activation (or disinhibition) of adenylate cyclase is necessary for the reduction in GABA current by CGP. Together, these data suggest that adenylate cyclase is normally inhibited by tonic GABA<sub>B</sub>R activity, but becomes disinhibited/activated when GABA<sub>B</sub>Rs are blocked by CGP.

How does activation of adenylate cyclase result in reduced GABA<sub>A</sub>R currents? Previous reports have shown that several conserved intracellular serine or tyrosine residues on GABA<sub>A</sub>R subunits are phosphorylation sites for kinases, including PKA, PKC, and CaMKII<sup>41–44</sup>. Phosphorylation of these residues maintains surface expression of GABA<sub>A</sub>Rs, whereas, dephosphorylation of these subunits triggers receptor internalization<sup>45,46</sup>. We first tested whether PKA is required for GABA<sub>A</sub>R enhancement by GABA<sub>B</sub>Rs, as it is a primary target of adenylate cyclase/cAMP activity. To block PKA activity we included the PKA inhibitory peptide PKI 14–22 ( $1 \mu\text{M}$ ) in the intracellular pipette solution. In the presence of this inhibitor the effects of CGP were highly variable. Overall, the change in uncaging current amplitude was not significant ( $80.1 \pm 10.9\%$  of control,  $n = 8$ ,  $p = 0.26$ ; Fig. 4C), suggesting PKA activity may be required for the effect of CGP on the GABA current. This is consistent with previous findings in many cells that PKA is normally inhibited by G<sub>i/o</sub> GPCRs (including GABA<sub>B</sub>Rs) and application of CGP results in activation/disinhibition of PKA<sup>37,38</sup>.

In order to identify other kinases involved in GABA<sub>B</sub>R-mediated modulation of the uncaging current, we next tested CaMKII and PKC. The inclusion of the PKC inhibitor GF-109203 ( $\times 1 \mu\text{M}$ ) in the bath solution did not inhibit the effects of CGP on the uncaging current ( $77.7 \pm 4.7\%$  of control,  $n = 6$ ,  $p = 0.01$ ; Fig. 4D). However, the inclusion of the CaMKII inhibitor KN-62 ( $2 \mu\text{M}$ ) in the bath solution abolished the effects of CGP on the uncaging current ( $90.9 \pm 7.9\%$  of control,  $n = 6$ ,  $p = 0.24$ , Fig. 4E). Furthermore, application of KN-62 alone was sufficient to reduce the uncaging current ( $68.5 \pm 5.3\%$  of control,  $n = 9$ ;  $p < 0.001$ ), indicating KN-62 mimics and occludes the effects of CGP. These data suggest that CGP reduces the uncaging current through inhibition of CaMKII.

CaMKII is regulated by intracellular calcium<sup>47,48</sup>, raising the possibility that the pathway from GABA<sub>B</sub>Rs to GABA<sub>A</sub>Rs involves changes in intracellular calcium. To test this we bath applied the cell permeable calcium chelator EGTA-AM, which becomes enriched inside the cell due to cleavage of the AM group. Application of  $20 \mu\text{M}$  EGTA-AM alone was sufficient to reduce uncaging current amplitudes ( $77.21 \pm 2.86\%$  of control,  $n = 9$ ,  $p < 0.001$ ; Fig. 5A). In the presence of EGTA-AM, further application of CGP had only a small effect on the current amplitude ( $88.92 \pm 3.33\%$  of EGTA-AM,  $n = 9$ ,  $p = 0.007$ ), possibly due to continued accumulation of EGTA inside the cell. When using a high EGTA ( $10 \text{ mM}$ ) internal solution, CGP application had no effect on GABA<sub>A</sub>R current amplitudes ( $105.97\% \pm 5.52$  of control,  $n = 9$ ,  $p = 0.43$ ; Fig. 5B). Furthermore, in slices bathed in calcium-free ACSF, application of CGP did not alter the uncaging current amplitude ( $98.1 \pm 2.04\%$  of control,  $n = 5$ ,  $p = 0.26$ ; Fig. 5C). These data suggest that changes in intracellular  $\text{Ca}^{+2}$  are required for enhancement of GABA<sub>A</sub>Rs by GABA<sub>B</sub>Rs.

Two primary sources of intracellular calcium are voltage-gated calcium channels and calcium release from intracellular stores. We first tested whether  $\text{Ca}^{+2}$  influx through L-type calcium channels is necessary for the CGP effect, as these channels make up approximately 90% of voltage-gated calcium channels (VGCC) in granule cell bodies<sup>49</sup>. In the presence of nifedipine (an L-type channel blocker), we still observed a significant reduction of the uncaging current amplitude following application of CGP ( $74.6 \pm 4.6\%$  of nifedipine,  $n = 9$ ,  $p = 0.003$ ), suggesting L-type calcium channels are not necessary for the effects of CGP. We then tested whether calcium release from intracellular stores is necessary for the effects of CGP. In slices preincubated in dantrolene ( $10 \mu\text{M}$ ), uncaging currents were not altered by application of CGP ( $95.83 \pm 4.8\%$  of control,  $n = 7$ ,  $p = 0.85$ ; Fig. 5F), confirming that ryanodine receptor-mediated release of calcium from intracellular stores is required for the effects of CGP on GABA<sub>A</sub>Rs. These data suggest that increases in intracellular calcium from intracellular stores can activate CaMKII and enhance GABA<sub>A</sub>R-mediated currents.

## Discussion

We find that GABA<sub>B</sub>Rs in cerebellar granule cells are tonically active and selectively enhance currents through extrasynaptic (presumably  $\delta$ -subunit containing) GABA<sub>A</sub>Rs. Blocking GABA<sub>B</sub>Rs reduces the number of GABA<sub>A</sub> channels activated by GABA, due to changes in desensitization and trafficking of receptors. Further, we find that GABA<sub>B</sub>R-mediated enhancement of GABA<sub>A</sub>Rs is dependent on signaling pathways including adenylate cyclase, PKA, CaMKII, and release of calcium from intracellular stores. Identification of the biophysical mechanisms and signaling pathway involved in regulation of tonic GABA<sub>A</sub>R currents will be important for understanding how ambient GABA and tonic inhibition in the granule cell layer regulates activity at the input layer of the cerebellum. Furthermore, the same mechanisms and pathways are likely employed in other cell types expressing extrasynaptic  $\delta$ -GABA<sub>A</sub>Rs, including thalamic relay neurons and dentate granule cells of the hippocampus. Our recent studies show that presynaptic GABA<sub>B</sub>Rs can also modulate GABA<sub>A</sub>Rs expressed in the presynaptic terminals of parallel fibers<sup>19,20</sup>. Many other presynaptic terminals throughout the central nervous system also co-express GABA<sub>A</sub> and

	Rise-time (ms)	Tau decay (ms)	Peak (CGP/cnt)
Expmt. (cnt)	24.9 ± 5.1	719.3 ± 101.3	
Expmt. (CGP)	17.6 ± 3.1	497.0 ± 68.0	61.6 ± 3.9
Model ( $d_2 = 0.02$ )	46.1	677.9	
Model ( $d_2 = 0.1$ )	38.7	439.1	75.5

**Table 1.** Kinetic parameters of experimentally recorded and simulated GABA<sub>A</sub>R currents.

GABA<sub>B</sub>Rs, raising the possibility that GABA<sub>B</sub>R-mediated enhancement of GABA<sub>A</sub>Rs is a widespread mechanism of synaptic modulation in presynaptic terminals.

**Tonic GABA<sub>B</sub> receptor activity.** The granule cell layer maintains basal levels of ambient GABA providing an additional layer of inhibition through extrasynaptic GABA<sub>A</sub>Rs<sup>6,50,51</sup>. While many studies have shown that ambient GABA tonically activates GABA<sub>A</sub>Rs in granule cells, tonic activation of GABA<sub>B</sub>Rs has received relatively little attention. Estimates of the GABA EC<sub>50</sub> for GABA<sub>B</sub>Rs can vary widely, however, several reports put this value in the low nanomolar range (5–20 nM<sup>38,52,53</sup>), well within the range for activation by ambient GABA (150–250 nM<sup>5,54</sup>). We have recently shown that GABA<sub>B</sub>Rs in the axons of granule cells respond to lower concentrations of GABA than GABA<sub>A</sub>Rs<sup>19</sup>, suggesting GABA<sub>B</sub>Rs may also be tonically activated in granule cells. This possibility is further supported by findings that GABA<sub>B</sub>Rs expressed on synaptic terminals of Golgi cells are tonically activated<sup>24</sup>. In this study, we find that application of a GABA<sub>B</sub>R antagonist alone is sufficient to reduce tonic GABA/muscimol evoked GABA<sub>A</sub>R currents (Figs 1H, 2B), suggesting GABA<sub>B</sub>Rs are constitutively activated. In addition, application of a GABA<sub>B</sub>R agonist, baclofen, does not alter the uncaging GABA current, consistent with prior activation of GABA<sub>B</sub>Rs by ambient GABA. These results differ from an earlier study which showed that baclofen increases the tonic current in cerebellar granule cells while CGP slightly decreases the tonic current<sup>17</sup>. These conflicting results may be due to the fact that the previous study used tetrodotoxin to block neuronal activity, shown to lower the level of ambient GABA in the granule cell layer at this age<sup>6,55</sup>, and limiting tonic GABA<sub>B</sub>R activity.

**Biophysical mechanisms of GABA<sub>A</sub> receptor enhancement.** There are several biophysical mechanisms that can account for changes in GABA<sub>A</sub>R-mediated currents, including changes in chloride reversal potential, GABA potency, channel open time, desensitization, single channel conductance, channel open probability, or the number of channels in the membrane. Recent work has shown that GABA<sub>B</sub>Rs can regulate the chloride transporter KCC2 altering the chloride reversal potential in neurons<sup>56</sup>. However, this is unlikely to account for the change in uncaging current in our experiments as the chloride reversal potential is determined by the relative chloride concentrations in the internal and bath solutions. We did not find changes in GABA potency (Fig. 3B), single channel conductance, or open probability (Fig. 3F). However, our data does suggest changes in channel gating contribute to the effects of blocking GABA<sub>B</sub>Rs. We observed a consistent decrease in the fast mean open time of the channel (Fig. 3D) and increased desensitization following GABA application (Fig. 3G), which may account for the increased rise-time and decay kinetics of the macroscopic GABA current. In a computer model of GABA<sub>A</sub>R gating we tested whether increasing the rate of desensitization could account for these changes and found that this change alone was sufficient to reduce the peak current amplitude, the rise-time, and the decay time. However, the fast open time account for only 3–5% of current fluctuations and the change in desensitized receptors was relatively small (5–10%), suggesting other mechanisms may also contribute to the relatively large change in the uncaging current. Using non-stationary fluctuation analysis we found that the number of channels participating in the GABA current was significantly reduced by CGP application (Fig. 3F). This decrease in available channels can be explained, at least in part, by increased accumulation of receptors into long-lasting desensitized states in response to low levels of ambient GABA, as has been reported at other GABA<sub>A</sub>Rs<sup>5,31</sup>. The literature on desensitization of  $\delta$ -subunit containing GABA<sub>A</sub>Rs has been mixed. Initial reports suggest these receptors show little or no desensitization<sup>32</sup>. More recent studies using  $\alpha_6\beta_{2/3}\delta$  receptors (the subunit composition thought to mediate the tonic current in cerebellar granule cells) or extrasynaptic receptors in granule cells suggest moderate to profound desensitization of these receptors<sup>2,5,33,34</sup>. However, changes in receptor trafficking and surface expression may also be necessary to account for the 40–50% reduction of the macroscopic GABA<sub>A</sub>R current. We therefore argue that GABA<sub>B</sub>R activity/blockade also alters trafficking and surface expression of GABA<sub>A</sub>Rs. Previous studies provide ample evidence that phosphorylation of GABA<sub>A</sub>Rs by common kinases (CaMKII, PKA, PKC) can alter GABA<sub>A</sub>R trafficking and surface expression<sup>41–44</sup>.

**Signaling mechanisms of GABA<sub>A</sub>R enhancement.** The primary signaling pathways of GABA<sub>B</sub>Rs, like all G<sub>i/o</sub> coupled GPCRs, is through inhibition of adenylate cyclase and reduction of cAMP production<sup>37,38</sup>. In our experiments, GABA<sub>B</sub>Rs are tonically activated, thus application of the GABA<sub>B</sub>R antagonist, CGP-55845, would disinhibit (or activate) adenylate cyclase and cAMP production. Consistent with this, we find that forskolin, an activator of adenylate cyclase, mimics and occludes the effects of CGP. Further, in the presence of SQ 22536, an adenylate cyclase inhibitor, CGP has no effect on the GABA<sub>A</sub>R current because there is no disinhibition of adenylate cyclase in this case. One of the main targets of cAMP in intracellular signaling cascade is PKA, thus disinhibition (or activation) of adenylate cyclase/cAMP production would activate PKA<sup>37,38</sup>. Consistent with this, we find that if activation of PKA is prevented by including a PKA inhibitory peptide in the intracellular solution, application of CGP does not significantly reduce the GABA<sub>A</sub>R current. This suggests activation of PKA is required for the CGP effect, and is consistent with earlier findings that PKA activity decreases tonic GABA<sub>A</sub>R currents in thalamo-cortical neurons<sup>17</sup>. However, phosphorylation of GABA<sub>A</sub>Rs by PKA can either increase or decrease

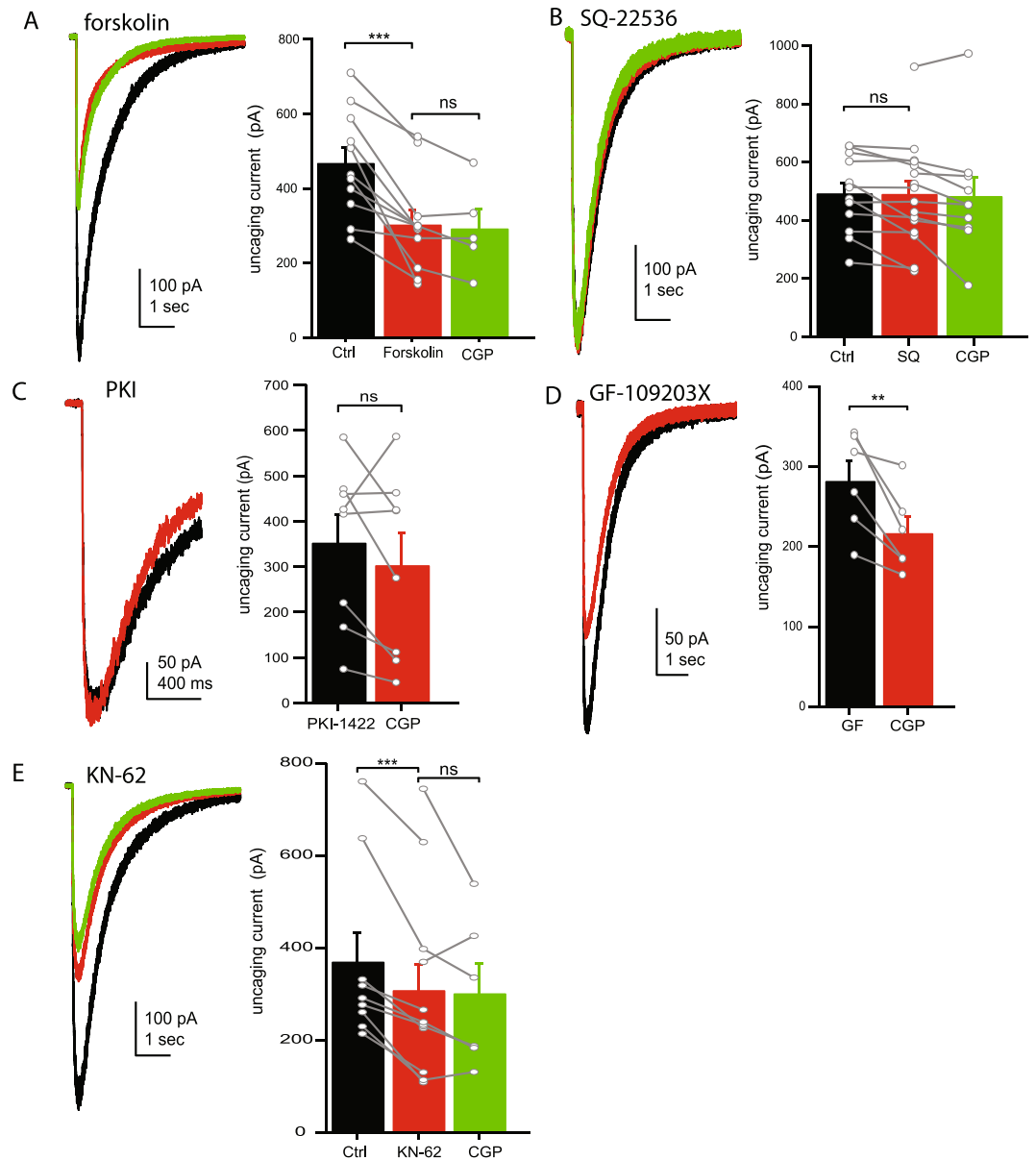


**Figure 4.** Intracellular kinase dependent enhancement of GABA<sub>A</sub>Rs. (A) Representative uncaging current traces (left) and average current amplitudes (right) in control ACSF (black), in the presence of the adenylate cyclase activator, forskolin (red) and following the addition of CGP55845 (green). (B) Representative uncaging current traces (left) and average current amplitudes (right) in control ACSF (black), in the presence of the adenylate cyclase inhibitor, SQ-22536 (red) and in the presence of CGP55845 (green). (C) Representative uncaging current traces (left) and average current amplitudes (right) in control ACSF (black) and in the presence of CGP55845 (red) when the PKA inhibitor, PKI 14–22, is included in the internal solution. (D) Representative uncaging current traces (left) and average current amplitudes (right) in control ACSF (black) and in the presence of CGP55845 (red) when the PKC inhibitor GF-109203X is included in the bath solution. (E) Representative uncaging current traces (left) and average current amplitudes (right) in control ACSF (black), in the presence of the CaMKII inhibitor, KN-62 (red) and following the addition of CGP55845 (green). Data from individual cells are plotted as connected gray markers. (\*\*) indicates  $p$ -value  $\leq 0.01$ , (\*\*\*) indicates  $p$ -value  $\leq 0.001$ , ns indicates  $p$ -value  $> 0.05$ .

surface expression of receptors depending on  $\beta$  subunit expression ( $\beta_1$  subunit containing receptor expression is decreased while  $\beta_3$  subunit containing receptor expression is increased)<sup>43,44,57</sup>. Cerebellar granule cells primarily express  $\beta_2$  and  $\beta_3$ , though  $\beta_1$  expression is also present at lower levels<sup>58,59</sup>. This suggests phosphorylation of GABA<sub>A</sub>Rs by PKA would primarily increase GABA<sub>A</sub>R expression, while we find that disinhibition/activation of PKA results in reduced GABA<sub>A</sub>R-mediated currents. It is therefore unlikely that PKA activity is directly involved in phosphorylating GABA<sub>A</sub>Rs. Rather, other signaling molecules/kinases must be involved.

Several studies have shown that CaMKII and PKC can also phosphorylate GABA<sub>A</sub>Rs and increase cell surface expression<sup>41,60–62</sup>. In cell expression system or in cerebellar granule cells, activation of CaMKII enhanced surface

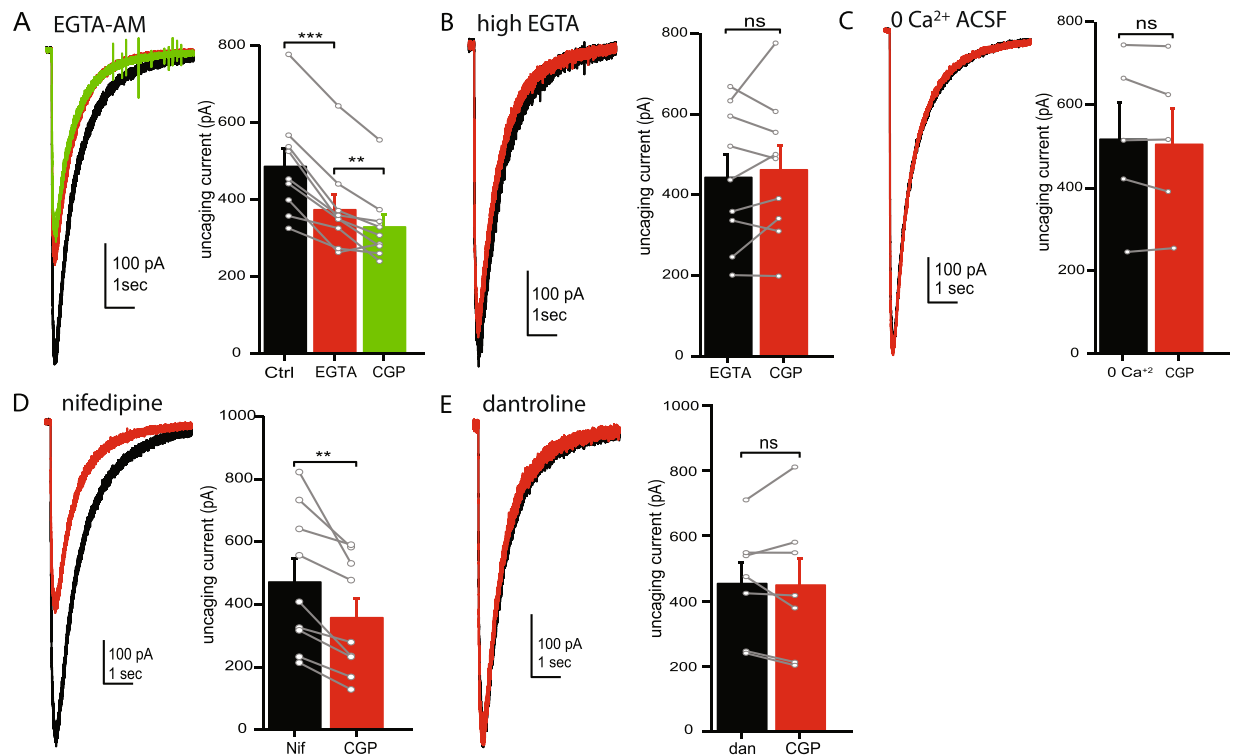


**Figure 5.** Intracellular calcium dependent enhancement of GABA<sub>A</sub>Rs. (A) Representative uncaging current traces (left) and average current amplitudes (right) in control ACSF (black), in the presence of the EGTA-AM (red) and following the addition of CGP55845 (green). (B) Representative uncaging current traces (left) and average current amplitudes (right) in control ACSF (black) and in the presence of CGP55845 (red) when high (10 mM) EGTA is included in the internal solution. (C) Representative uncaging current traces (left) and average current amplitudes (right) in 0 calcium ACSF (black) and following application of CGP55845 (red). (D) Representative uncaging current traces (left) and average current amplitudes (right) in the presence of nifedipine (black), and following addition of CGP55845 (red). (E) Representative uncaging current traces (left) and average current amplitudes (right) in the presence of dantrolene (black) and following addition of CGP55845 (red). Data from individual cells are plotted as connected gray markers. (\*\*) indicates  $p$ -value  $\leq 0.01$ , (\*\*\*) indicates  $p$ -value  $\leq 0.001$ , ns indicates  $p$ -value  $> 0.05$ .

expression of GABA<sub>A</sub>Rs containing a  $\beta 3$  subunit but not receptors containing a  $\beta 2$  subunit<sup>47</sup>. Furthermore, the expression of  $\beta 3$  subunits may contribute to receptor trafficking and the cellular location of receptor expression<sup>63</sup>. In our experiments blocking CaMKII, but not PKC, abolished the effect of CGP application on GABA<sub>A</sub>R currents. In fact, application of KN-62 (a CaMKII inhibitor) alone was sufficient to reduce the GABA<sub>A</sub>R current, suggesting that CGP acts through inhibition of CaMKII. This raises the possibility that GABA<sub>B</sub>R modulation acts through CaMKII dependent phosphorylation of extrasynaptic, but not synaptic receptors, based on  $\beta$  subunit expression.

CaMKII activity is highly dependent on calcium, raising the possibility that changes in intracellular calcium levels are involved in the CGP effect. Indeed, we find that the effects of CGP are absent in the presence of high EGTA or following removal of extracellular calcium (Fig. 5B,C). There are two primary sources of intracellular calcium in neurons, influx of calcium through voltage-gated calcium channels and release of calcium from intracellular stores. Inhibition of calcium release from intracellular stores, but not inhibition of L-type calcium channels (which constitute ~90% of voltage-gated calcium channels in granule cells<sup>49</sup>), abolished the effects of CGP (Fig. 5F), suggesting calcium release from intracellular stores is more important than calcium influx for this effect. However, the observation that the CGP effect is abolished by removal of calcium from the bath solution suggests influx of calcium may also be necessary. It is tempting to speculate that calcium influx (through channels other than L-type channels) induces calcium release from intracellular stores. However, mature granule cells show little evidence of calcium induced calcium release<sup>64–66</sup>, suggesting this is not the case. Another possibility is that bathing the slice in 0 Ca<sup>2+</sup> aCSF results in a slow depletion of intracellular stores, and subsequent loss of the CGP effect.

The requirement of release of calcium from intracellular stores would seem to implicate G<sub>q</sub> coupled receptors, not G<sub>i/o</sub> coupled receptors such as the GABA<sub>B</sub>R, which signal primarily through adenylate cyclase and cAMP. However, a number of previous studies have also observed a rise in calcium from intracellular stores as a result of GABA<sub>B</sub>R activation in a variety of cells<sup>67–69</sup> including cerebellar granule cells<sup>70</sup>. While the entire signaling pathway remains unclear, it has been shown to depend on signaling through IP<sub>3</sub> and IP<sub>3</sub> receptors<sup>71</sup>. One possible mechanism is through activity of the G <sub>$\beta_1$</sub>  subunit, which has been shown to stimulate PLC $\beta_1$ –3<sup>72</sup> and/or formation of IP<sub>3</sub><sup>73–75</sup>. This raises the possibility that GABA<sub>B</sub>Rs signal through PKA with the G <sub>$\alpha$</sub>  subunit and stimulate release of calcium from intracellular stores with the G <sub>$\beta_1$</sub>  subunit. While this possibility is consistent with our data, we do not have any direct evidence of GABA<sub>B</sub>R-mediated activation of PLC or formation of IP<sub>3</sub>.



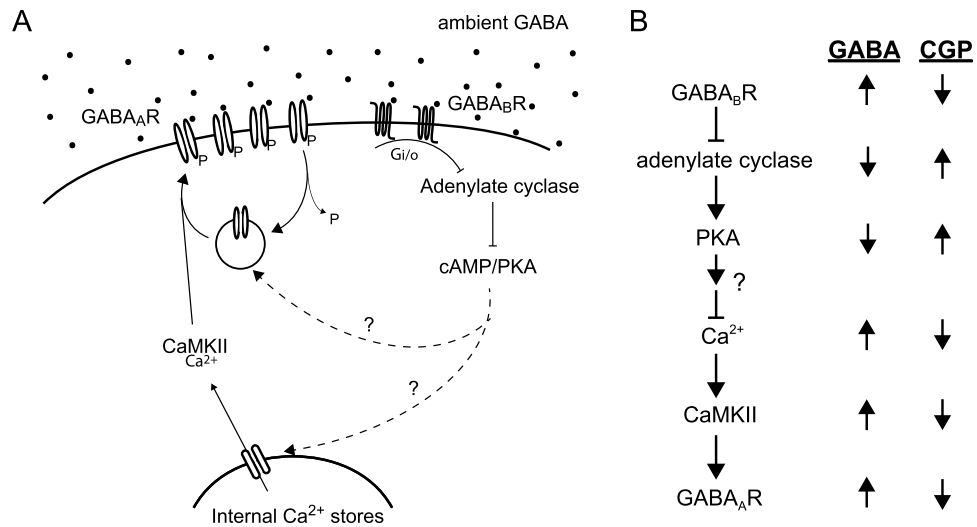


**Figure 6.** GABA<sub>B</sub>R signaling model. (A) Diagram of the signaling mechanism linking GABA<sub>B</sub>R activation to enhancement of extrasynaptic GABA<sub>A</sub>Rs. (B) Chart indicating predicted changes at each step in the signaling pathway when GABA<sub>B</sub>Rs are activated (GABA) or inhibited (CGP).

Based on our data we propose a signaling pathway following GABA<sub>B</sub>R activation involving inhibition of adenylate cyclase and PKA (Fig. 6). This directly or indirectly produces a downstream increase in calcium release from intracellular stores and activation of CaMKII. Finally, CaMKII phosphorylates extrasynaptic GABA<sub>A</sub>Rs resulting in decreased desensitization and/or insertion of receptors into the surface membrane.

**Physiological relevance.** The granule cell layer is the primary input layer of the cerebellum, where granule cells integrate and process information received from across many brain regions<sup>76</sup>. Spike processing in granule cells is influenced by phasic inhibition from Golgi cell terminals, and tonic inhibition mediated by extrasynaptic GABA<sub>A</sub>Rs. It has been estimated that tonic inhibition accounts for 25–75% of chloride influx in granule cells<sup>77</sup> and regulates the gain of the input/output function of these cells<sup>78</sup>. Previous work has shown that the level of ambient GABA in the cerebellum can be modulated, affecting granule cell firing and cerebellar function. For example, neuroinflammation in the cerebellum has been shown to increase ambient GABA, resulting in impaired motor coordination<sup>79</sup>. Our data suggest that GABA<sub>B</sub>R enhancement of GABA<sub>A</sub>Rs may amplify the effects of ambient GABA on granule cell firing. Low levels of ambient GABA likely produce little activation of GABA<sub>A</sub> or GABA<sub>B</sub>Rs, resulting in little or no tonic GABA<sub>A</sub>R current. However, as the ambient GABA concentration increases the tonic GABA<sub>A</sub>R current is expected to increase due to both direct activation of GABA<sub>A</sub>Rs and due to increased activation of GABA<sub>B</sub>Rs and the resulting enhancement of extrasynaptic GABA<sub>A</sub>Rs. This creates a much steeper response of GABA<sub>A</sub>Rs to changes in ambient GABA than would be expected from the biophysical properties of the GABA<sub>A</sub>Rs alone and increases the sensitivity of granule cells to changes in ambient GABA.

**Future directions.** Cerebellar granule cells express a range of G-protein coupled receptors including, GABA<sub>B</sub>Rs<sup>80</sup>, adenosine A1 receptors<sup>81</sup>, orexin receptors<sup>82</sup>, and glutamate receptors (mGluRs)<sup>83</sup>. This raises the question of whether modulation of extrasynaptic GABA<sub>A</sub>Rs is specific to GABA<sub>B</sub>Rs in these cells or if other types of G-protein coupled receptors can also activate/inhibit this pathway. It was recently shown that orexin receptors (OX1 and OX2) are expressed in granule cells and their activation decreases GABA<sub>A</sub>R-mediated currents in a calcium dependent manner<sup>82</sup>. This suggests that orexin receptors may employ the same mechanisms as GABA<sub>B</sub>Rs to modulate GABA<sub>A</sub>R function, though in the opposite direction. The opposite effect of orexin receptors on GABA<sub>A</sub>R-mediated currents may be accounted for by the fact that orexin receptors couple to G<sub>s</sub> subunits (in addition to G<sub>i/o</sub> and G<sub>q</sub>)<sup>84</sup> which generally activate adenylate cyclase, unlike G<sub>i/o</sub> subunits which inhibit adenylate cyclase. These data suggests that orexin receptors, and possibly other G<sub>s</sub> coupled receptors, may regulate tonic GABA<sub>A</sub>R-mediated currents in opposition to GABA<sub>B</sub>Rs using the same signaling pathways. Future experiments will be required to determine if other G-protein coupled receptors, besides GABA<sub>B</sub>Rs, also employ the signaling pathway/biophysical mechanisms to regulate GABA<sub>A</sub>Rs.

Our results indicate that only extrasynaptic receptors in granule cells are modulated by GABA<sub>B</sub>R activity. This result is consistent with  $\delta$ -subunit expression patterns, but does not directly implicate these receptors. It remains possible that the  $\delta$ -subunit itself is not necessary for this form of modulation and other extrasynaptic receptors lacking the  $\delta$ -subunit can also be modulated by this mechanism. In the future these questions can be addressed using cell-type specific  $\delta$ -subunit knock-out mice.

## Experimental Procedures

**Animals.** All experimental procedures involving animals were approved by the Institutional Animal Care and Use Committee at UT Health San Antonio and followed the guidelines of the *National Institutes of Health's Guide for the Care and Use of Laboratory Animals*. Male and female C57BL/6 mice (Charles River, MA) 14–30 days old were used for all experiments. Animals were kept on a 12/12 hour light dark cycle with *ad libitum* access to food and water.

**Slice preparation.** Mice were deeply anesthetized with isoflurane and the cerebellum was rapidly dissected following decapitation and placed in ice-cold oxygenated ACSF containing the following (in mM): 119 NaCl, 26.2 NaHCO<sub>3</sub>, 2.5 KCl, 1.0 NaH<sub>2</sub>PO<sub>4</sub>, 11 glucose, 2 CaCl<sub>2</sub>, 1.3 MgCl<sub>2</sub> as described previously<sup>19</sup>. Parasagittal slices (250–300 μm) were cut from the vermis of the cerebellum using a vibratome (Leica Biosystems, IL) and then incubated at 34 °C for 30 min, after which they were used for electrophysiological recordings at room temperature.

**Electrophysiology experiments.** For recording, slices were gently placed in a chamber that was perfused with room temperature ACSF containing the following (in mM): 119 NaCl, 26.2 NaHCO<sub>3</sub>, 2.5 KCl, 1.0 NaH<sub>2</sub>PO<sub>4</sub>, 11 glucose, 2 CaCl<sub>2</sub>, 1.3 MgCl<sub>2</sub> (flow rate of ~2 ml/min) housed in a SliceScope Pro upright microscope (Scientifica Instruments, UK.). For experiments on somatodendritic GABA currents, whole cell patch clamp recordings were made from granule cells, Purkinje cells, and stellate cells with the following internal (in mM): 135 CsCl, 10 HEPES, 4 MgCl<sub>2</sub>, 5 EGTA, 4 Na-ATP, 0.5 Na-GTP, 2 QX-314. Additional drugs were included in the internal solution as indicated in the text. The pH of the internal solution was adjusted to 7.2–7.4 using CsOH and the osmolarity was 280–300 mosmol. Cells were patched using 4–6 MΩ borosilicate glass pipettes (Sutter instruments) that were pulled on Sutter pipette puller (Model P-100, Sutter instruments, CA, USA). Electrophysiological currents were recorded with a Multiclamp 700B amplifier (Molecular Devices, CA), filtered at 5 kHz and digitized at 50 kHz. Data were collected using pCLAMP software (Molecular Devices). For GABA uncaging experiments, 10 ml of ACSF containing 10 μM NBQX (Tocris, MN) and 60 μM RuBi-GABA (Tocris) was recirculated using a fluid pump (Cole-Parmer, IL). RuBi-GABA at this concentration does not alter membrane resistance of the cell<sup>20</sup>. GABA was uncaged by a brief (5 ms) illumination from a 470 nm light-emitting diode (LED) (CoolLED, Andover, UK) at 20% intensity (resulting in ~4 μM free GABA<sup>19</sup>) to preferentially activate high-affinity extrasynaptic GABA<sub>A</sub>Rs. We used a 30 second inter-sweep interval to allow for clearance of GABA between sweeps. For GABA dose-response experiments a 473 nm laser light source (PSU-III-LED, Opto Engine LLC, Midvale, UT) was used for GABA uncaging. The laser power was modulated over a range of intensities (0.28 μW–315 μW) to modulate the amount of GABA released. The maximum GABA concentration in these experiments was not more than 60 μM (the concentration of RuBi-GABA in the bath) and likely much less (20–40 μM). For this reason the saturation of responses at high laser powers likely represents saturation of GABA uncaging rather than saturation of GABA<sub>A</sub> receptors. The uncaging laser intensity was measured using a photometer placed under the objective of the microscope. For each experiment uncaging current amplitudes were first measured over 3–5 minutes to obtain a stable baseline amplitude before adding CGP55845 or other drugs. Cells in which the uncaging current amplitude was not stable over this period were not included for further analysis. The tonic GABA<sub>A</sub> current in granule cells was measured by the net change in holding current following application of 20 μM bicuculline (Tocris, MN). In tonic current recordings the ACSF contained 10 μM NBQX and 10 μM CPP. Access resistances of all cells were monitored and cells deviating from 20 ± 10 MΩ were discarded.

Where indicated, ACSF contained one or more of the following: 3 μM CGP 55845 (CGP, Abcam, Cambridge, MA, USA); 200 μM picrotoxin (PTX; Abcam); 200 μM 2-hydroxysaclofen (Tocris); 20 μM Bicuculline (Tocris), 100 μM Baclofen (Abcam), 10 μM NN711, 1 mM GDP-β-S (Sigma), 10 μM Forskolin (sigma), 100 μM SQ-22536 (Tocris), 1 μM PKI 14–22, 1 μM GF-109203 ×, 3–6 μM Nifedipine (Tocris), 2 μM KN-62 (Tocris), 20 μM EGTA-AM (Tocris), or 10 μM Dantrolene (Tocris).

**Data analysis.** Data were analyzed using IgorPro (Wavemetrics, Lake Oswego, OR, USA) using the Neuromatic plug-in<sup>85</sup> and Excel (Microsoft, Redmond, WA, USA). Statistical significance was determined using 2-tailed paired Student's t-tests in Excel (Microsoft, Redmond, WA, USA) or Prism 6 (GraphPad Software, La Jolla, CA, USA). Statistical values of  $p \leq 0.05$  were considered significant.

**Power-spectra analysis:** In order to measure the power-spectra of GABA<sub>A</sub>R mediated currents, GABA was applied to cerebellar granule cells by prolonged uncaging of 60 μM RuBi-GABA (12 second pulse from 473 nm LED). GABA uncaging sweeps were interleaved with background sweeps in which the LED was not activated. GABA<sub>A</sub>R mediated currents were first recorded in standard ACSF and then following bath application of 3 μM CGP55845. For each sweep, the power spectra was computed by fast Fourier transform over 16 segments of 8192 points each and averaged. In order to avoid time dependent changes in current amplitude, the time segments analyzed began at 5 seconds after the onset of GABA uncaging where the macroscopic GABA current was relatively stable. The power spectra of interleaved background sweeps (lacking GABA uncaging) were computed by the same method and subtracted from GABA power spectra. The power spectra was fitted with the sum of three Lorentzian functions of the form:

$$L(f) = S/(1 + (2\pi * f * \tau)^2)$$

where  $L(f)$  is the spectral density at frequency  $f$ ,  $S$  is the power of the spectrum at  $f=0$ , and  $\tau$  is the time constant.

**Non-stationary fluctuation analysis:** GABA currents were recorded in cerebellar granule cells following either a brief (5 ms) puff of muscimol (10 μM) at the soma or uncaging of RuBi-GABA (60 μM) using a brief (5 ms) flash from a 473 nm laser. For each sweep, amplitude and variance were measured from the peak current to the end of the decay. The average current was scaled to the peak of each individual sweep and subtracted from the current trace, producing a difference trace for each sweep which was then squared to produce a variance trace. Each sweep was then divided into 30 equivalent amplitude bins and the mean current amplitude and variance were measured for each bin. The mean current was plotted against the mean variance and fitted with the following function:

$$\sigma^2 = iI_m - I_m^2/N$$

where  $\sigma^2$  is the variance,  $I_m$  is the mean current,  $i$  is the single channel current, and  $N$  is the number of channels participating in the current. For all cells included in the final data set the peak current was at least 60% (mean:  $78.2 \pm 5.2\%$ ) of the theoretical maximal current (the x-intercept in the variance equation above). The maximum open probability ( $P_{O_{max}}$ ) was calculated by dividing the peak current by ( $i \cdot N$ ), the x-intercept of the fitting function<sup>86</sup>.

**Modelling.** GABA<sub>A</sub>R-mediated currents evoked by GABA uncaging in cerebellar granule cells were modelled in NEURON<sup>87</sup>, based on a kinetic scheme first described by Jones and Westbrook<sup>35</sup>, consisting of single- and double-liganded closed, open, and desensitized states. The model was adapted from the granule cell model developed by Diwakar *et al.*<sup>88</sup>, and was obtained from ModelDB<sup>89</sup> (accession number 116835). GABA uncaging was modelled as a 5 ms square pulse of 60  $\mu$ M GABA followed by an exponential decay, to replicate the relatively low concentrations of GABA used in experiments. Transition rates were optimized to fit the rise-time and decay kinetics of the recorded currents.

## Data availability

We will make all materials, data and associated protocols derived from this work promptly available to other researchers without undue qualifications or delays.

Received: 31 July 2019; Accepted: 26 October 2019;

Published online: 13 November 2019

## References

- Essrich, C., Lorez, M., Benson, J. A., Fritschy, J. M. & Luscher, B. Postsynaptic clustering of major GABA<sub>A</sub> receptor subtypes requires the gamma 2 subunit and gephyrin. *Nature neuroscience* **1**, 563–571, <https://doi.org/10.1038/2798> (1998).
- Brickley, S. G., Cull-Candy, S. G. & Farrant, M. Single-channel properties of synaptic and extrasynaptic GABA<sub>A</sub> receptors suggest differential targeting of receptor subtypes. *The Journal of neuroscience: the official journal of the Society for Neuroscience* **19**, 2960–2973 (1999).
- Sun, M. Y. *et al.* Chemogenetic Isolation Reveals Synaptic Contribution of delta GABA<sub>A</sub> Receptors in Mouse Dentate Granule Neurons. *The Journal of neuroscience: the official journal of the Society for Neuroscience* **38**, 8128–8145, <https://doi.org/10.1523/JNEUROSCI.0799-18.2018> (2018).
- Wei, W., Zhang, N., Peng, Z., Houser, C. R. & Mody, I. Perisynaptic localization of delta subunit-containing GABA(A) receptors and their activation by GABA spillover in the mouse dentate gyrus. *The Journal of neuroscience: the official journal of the Society for Neuroscience* **23**, 10650–10661 (2003).
- Bright, D. P. *et al.* Profound desensitization by ambient GABA limits activation of delta-containing GABA<sub>A</sub> receptors during spillover. *The Journal of neuroscience: the official journal of the Society for Neuroscience* **31**, 753–763, <https://doi.org/10.1523/JNEUROSCI.2996-10.2011> (2011).
- Brickley, S. G., Cull-Candy, S. G. & Farrant, M. Development of a tonic form of synaptic inhibition in rat cerebellar granule cells resulting from persistent activation of GABA<sub>A</sub> receptors. *The Journal of physiology* **497**(Pt 3), 753–759 (1996).
- Mitchell, S. J. & Silver, R. A. Shunting inhibition modulates neuronal gain during synaptic excitation. *Neuron* **38**, 433–445 (2003).
- Meera, P., Wallner, M. & Otis, T. S. Molecular basis for the high THIP/gaboxadol sensitivity of extrasynaptic GABA(A) receptors. *Journal of neurophysiology* **106**, 2057–2064, <https://doi.org/10.1152/jn.00450.2011> (2011).
- Houston, C. M. *et al.* Are extrasynaptic GABA<sub>A</sub> receptors important targets for sedative/hypnotic drugs? *The Journal of neuroscience: the official journal of the Society for Neuroscience* **32**, 3887–3897, <https://doi.org/10.1523/JNEUROSCI.5406-11.2012> (2012).
- Hanchar, H. J., Dodson, P. D., Olsen, R. W., Otis, T. S. & Wallner, M. Alcohol-induced motor impairment caused by increased extrasynaptic GABA(A) receptor activity. *Nature neuroscience* **8**, 339–345, <https://doi.org/10.1038/nn1398> (2005).
- Santhakumar, V., Wallner, M. & Otis, T. S. Ethanol acts directly on extrasynaptic subtypes of GABA<sub>A</sub> receptors to increase tonic inhibition. *Alcohol* **41**, 211–221, <https://doi.org/10.1016/j.alcohol.2007.04.011> (2007).
- Diaz, M. R. & Valenzuela, C. F. Sensitivity of GABAergic Tonic Currents to Acute Ethanol in Cerebellar Granule Neurons is Not Age- or delta Subunit-Dependent in Developing Rats. *Alcoholism, clinical and experimental research* **40**, 83–92, <https://doi.org/10.1111/acer.12940> (2016).
- Borghese, C. M. & Harris, R. A. Studies of ethanol actions on recombinant delta-containing gamma-aminobutyric acid type A receptors yield contradictory results. *Alcohol* **41**, 155–162, <https://doi.org/10.1016/j.alcohol.2007.03.006> (2007).
- Brickley, S. G. & Mody, I. Extrasynaptic GABA(A) receptors: their function in the CNS and implications for disease. *Neuron* **73**, 23–34, <https://doi.org/10.1016/j.neuron.2011.12.012> (2012).
- Maguire, J. L., Stell, B. M., Rafizadeh, M. & Mody, I. Ovarian cycle-linked changes in GABA(A) receptors mediating tonic inhibition alter seizure susceptibility and anxiety. *Nature neuroscience* **8**, 797–804, <https://doi.org/10.1038/nn1469> (2005).
- Stell, B. M., Brickley, S. G., Tang, C. Y., Farrant, M. & Mody, I. Neuroactive steroids reduce neuronal excitability by selectively enhancing tonic inhibition mediated by delta subunit-containing GABA<sub>A</sub> receptors. *Proceedings of the National Academy of Sciences of the United States of America* **100**, 14439–14444, <https://doi.org/10.1073/pnas.2435457100> (2003).
- Connelly, W. M. *et al.* GABAB Receptors Regulate Extrasynaptic GABA<sub>A</sub> Receptors. *The Journal of neuroscience: the official journal of the Society for Neuroscience* **33**, 3780–3785, <https://doi.org/10.1523/JNEUROSCI.4989-12.2013> (2013).
- Tao, W., Higgs, M. H., Spain, W. J. & Ransom, C. B. Postsynaptic GABAB receptors enhance extrasynaptic GABA<sub>A</sub> receptor function in dentate gyrus granule cells. *The Journal of neuroscience: the official journal of the Society for Neuroscience* **33**, 3738–3743, <https://doi.org/10.1523/JNEUROSCI.4829-12.2013> (2013).
- Howell, R. D. & Pugh, J. R. Biphasic modulation of parallel fibre synaptic transmission by co-activation of presynaptic GABA<sub>A</sub> and GABAB receptors in mice. *The Journal of physiology* **594**, 3651–3666, <https://doi.org/10.1113/JP272124> (2016).
- Khatiri, S. N., Wu, W. C., Yang, Y. & Pugh, J. R. Direction of action of presynaptic GABA<sub>A</sub> receptors is highly dependent on the level of receptor activation. *Journal of neurophysiology*, <https://doi.org/10.1152/jn.00779.2018> (2019).
- Otis, T. S., De Koninck, Y. & Mody, I. Characterization of synaptically elicited GABAB responses using patch-clamp recordings in rat hippocampal slices. *The Journal of physiology* **463**, 391–407, <https://doi.org/10.1113/jphysiol.1993.sp019600> (1993).
- Alreja, M. & Aghajanian, G. K. QX-314 blocks the potassium but not the sodium-dependent component of the opiate response in locus coeruleus neurons. *Brain research* **639**, 320–324 (1994).
- Nusser, Z., Sieghart, W. & Somogyi, P. Segregation of different GABA<sub>A</sub> receptors to synaptic and extrasynaptic membranes of cerebellar granule cells. *The Journal of neuroscience: the official journal of the Society for Neuroscience* **18**, 1693–1703 (1998).
- Mapelli, L., Rossi, P., Nieuwe, T. & D'Angelo, E. Tonic activation of GABAB receptors reduces release probability at inhibitory connections in the cerebellar glomerulus. *Journal of neurophysiology* **101**, 3089–3099, <https://doi.org/10.1152/jn.91190.2008> (2009).

25. Chandra, D. *et al.* Prototypic GABA(A) receptor agonist muscimol acts preferentially through forebrain high-affinity binding sites. *Neuropsychopharmacology: official publication of the American College of Neuropsychopharmacology* **35**, 999–1007, <https://doi.org/10.1038/npp.2009.203> (2010).
26. Benkherouf, A. Y. *et al.* Extrasynaptic delta-GABAA receptors are high-affinity muscimol receptors. *Journal of neurochemistry* **149**, 41–53, <https://doi.org/10.1111/jnc.14646> (2019).
27. Kulik, A. *et al.* Distinct localization of GABA(B) receptors relative to synaptic sites in the rat cerebellum and ventrobasal thalamus. *The European journal of neuroscience* **15**, 291–307 (2002).
28. Traynelis, S. F. & Jaramillo, F. Getting the most out of noise in the central nervous system. *Trends in neurosciences* **21**, 137–145 (1998).
29. Alvarez, V. A., Chow, C. C., Van Bockstaele, E. J. & Williams, J. T. Frequency-dependent synchrony in locus ceruleus: role of electrotonic coupling. *Proceedings of the National Academy of Sciences of the United States of America* **99**, 4032–4036, <https://doi.org/10.1073/pnas.062716299> (2002).
30. Saviane, C. & Silver, R. A. Fast vesicle reloading and a large pool sustain high bandwidth transmission at a central synapse. *Nature* **439**, 983–987, <https://doi.org/10.1038/nature04509> (2006).
31. Overstreet, L. S., Jones, M. V. & Westbrook, G. L. Slow desensitization regulates the availability of synaptic GABA(A) receptors. *The Journal of neuroscience: the official journal of the Society for Neuroscience* **20**, 7914–7921 (2000).
32. Saxena, N. C. & Macdonald, R. L. Assembly of GABAA receptor subunits: role of the delta subunit. *The Journal of neuroscience: the official journal of the Society for Neuroscience* **14**, 7077–7086 (1994).
33. Wohlfarth, K. M., Bianchi, M. T. & Macdonald, R. L. Enhanced neurosteroid potentiation of ternary GABA(A) receptors containing the delta subunit. *The Journal of neuroscience: the official journal of the Society for Neuroscience* **22**, 1541–1549 (2002).
34. Feng, H. J., Botzolakis, E. J. & Macdonald, R. L. Context-dependent modulation of alphabeta gamma and alphabeta delta GABA A receptors by penicillin: implications for phasic and tonic inhibition. *Neuropharmacology* **56**, 161–173, <https://doi.org/10.1016/j.neuropharm.2008.08.010> (2009).
35. Jones, M. V. & Westbrook, G. L. Desensitized states prolong GABAA channel responses to brief agonist pulses. *Neuron* **15**, 181–191 (1995).
36. Pugh, J. R. & Raman, I. M. GABAA receptor kinetics in the cerebellar nuclei: evidence for detection of transmitter from distant release sites. *Biophysical journal* **88**, 1740–1754, <https://doi.org/10.1529/biophysj.104.055814> (2005).
37. Bettler, B., Kaupmann, K., Mosbacher, J. & Gassmann, M. Molecular structure and physiological functions of GABA(B) receptors. *Physiological reviews* **84**, 835–867, <https://doi.org/10.1152/physrev.00036.2003> (2004).
38. Bowery, N. G. *et al.* International Union of Pharmacology. XXXIII. Mammalian gamma-aminobutyric acid(B) receptors: structure and function. *Pharmacological reviews* **54**, 247–264 (2002).
39. Knight, A. R. & Bowery, N. G. The pharmacology of adenylyl cyclase modulation by GABAB receptors in rat brain slices. *Neuropharmacology* **35**, 703–712 (1996).
40. Xu, J. & Wojcik, W. J. Gamma aminobutyric acid B receptor-mediated inhibition of adenylate cyclase in cultured cerebellar granule cells: blockade by islet-activating protein. *The Journal of pharmacology and experimental therapeutics* **239**, 568–573 (1986).
41. Saliba, R. S., Kretschmannova, K. & Moss, S. J. Activity-dependent phosphorylation of GABAA receptors regulates receptor insertion and tonic current. *The EMBO journal* **31**, 2937–2951, <https://doi.org/10.1038/emboj.2012.109> (2012).
42. Brandon, N. J. *et al.* GABAA receptor phosphorylation and functional modulation in cortical neurons by a protein kinase C-dependent pathway. *The Journal of biological chemistry* **275**, 38856–38862, <https://doi.org/10.1074/jbc.M004910200> (2000).
43. McDonald, B. J. *et al.* Adjacent phosphorylation sites on GABAA receptor beta subunits determine regulation by cAMP-dependent protein kinase. *Nature neuroscience* **1**, 23–28, <https://doi.org/10.1038/223> (1998).
44. McDonald, B. J. & Moss, S. J. Conserved phosphorylation of the intracellular domains of GABA(A) receptor beta2 and beta3 subunits by cAMP-dependent protein kinase, cGMP-dependent protein kinase protein kinase C and Ca<sup>2+</sup>/calmodulin type II-dependent protein kinase. *Neuropharmacology* **36**, 1377–1385 (1997).
45. Kittler, J. T. *et al.* Regulation of synaptic inhibition by phospho-dependent binding of the AP2 complex to a YECL motif in the GABAA receptor gamma2 subunit. *Proceedings of the National Academy of Sciences of the United States of America* **105**, 3616–3621, <https://doi.org/10.1073/pnas.0707920105> (2008).
46. Kittler, J. T. *et al.* Phospho-dependent binding of the clathrin AP2 adaptor complex to GABAA receptors regulates the efficacy of inhibitory synaptic transmission. *Proceedings of the National Academy of Sciences of the United States of America* **102**, 14871–14876, <https://doi.org/10.1073/pnas.0506653102> (2005).
47. Houston, C. M. & Smart, T. G. CaMK-II modulation of GABA(A) receptors expressed in HEK293, NG108-15 and rat cerebellar granule neurons. *The European journal of neuroscience* **24**, 2504–2514, <https://doi.org/10.1111/j.1460-9568.2006.05145.x> (2006).
48. Fink, C. C. & Meyer, T. Molecular mechanisms of CaMKII activation in neuronal plasticity. *Current opinion in neurobiology* **12**, 293–299 (2002).
49. Koschak, A. *et al.* Molecular nature of anomalous L-type calcium channels in mouse cerebellar granule cells. *The Journal of neuroscience: the official journal of the Society for Neuroscience* **27**, 3855–3863, <https://doi.org/10.1523/JNEUROSCI.4028-06.2007> (2007).
50. Rossi, D. J., Hamann, M. & Attwell, D. Multiple modes of GABAergic inhibition of rat cerebellar granule cells. *The Journal of physiology* **548**, 97–110, <https://doi.org/10.1113/jphysiol.2002.036459> (2003).
51. Semyanov, A., Walker, M. C. & Kullmann, D. M. GABA uptake regulates cortical excitability via cell type-specific tonic inhibition. *Nature neuroscience* **6**, 484–490, <https://doi.org/10.1038/nn1043> (2003).
52. Bowery, N. G. GABAB receptor pharmacology. *Annual review of pharmacology and toxicology* **33**, 109–147, <https://doi.org/10.1146/annurev.pa.33.040193.000545> (1993).
53. Froestl, W. & Mickel, S. J. In *The GABA receptors* 271–296 (Springer, 1997).
54. Santhakumar, V., Hancher, H. J., Wallner, M., Olsen, R. W. & Otis, T. S. Contributions of the GABAA receptor alpha6 subunit to phasic and tonic inhibition revealed by a naturally occurring polymorphism in the alpha6 gene. *The Journal of neuroscience: the official journal of the Society for Neuroscience* **26**, 3357–3364, <https://doi.org/10.1523/JNEUROSCI.4799-05.2006> (2006).
55. Wall, M. J. & Usowicz, M. M. Development of action potential-dependent and independent spontaneous GABAA receptor-mediated currents in granule cells of postnatal rat cerebellum. *The European journal of neuroscience* **9**, 533–548 (1997).
56. Wright, R. *et al.* Neuronal Chloride Regulation via KCC2 Is Modulated through a GABAB Receptor Protein Complex. *The Journal of neuroscience: the official journal of the Society for Neuroscience* **37**, 5447–5462, <https://doi.org/10.1523/JNEUROSCI.2164-16.2017> (2017).
57. Moss, S. J. & Smart, T. G. Modulation of amino acid-gated ion channels by protein phosphorylation. *International review of neurobiology* **39**, 1–52 (1996).
58. Wisden, W., Korpi, E. R. & Bahn, S. The cerebellum: a model system for studying GABAA receptor diversity. *Neuropharmacology* **35**, 1139–1160 (1996).
59. Nusser, Z., Roberts, J. D., Baude, A., Richards, J. G. & Somogyi, P. Relative densities of synaptic and extrasynaptic GABAA receptors on cerebellar granule cells as determined by a quantitative immunogold method. *The Journal of neuroscience: the official journal of the Society for Neuroscience* **15**, 2948–2960 (1995).
60. Houston, C. M., Hosie, A. M. & Smart, T. G. Distinct regulation of beta2 and beta3 subunit-containing cerebellar synaptic GABAA receptors by calcium/calmodulin-dependent protein kinase II. *The Journal of neuroscience: the official journal of the Society for Neuroscience* **28**, 7574–7584, <https://doi.org/10.1523/JNEUROSCI.5531-07.2008> (2008).



61. Lin, Y. F., Angelotti, T. P., Dudek, E. M., Browning, M. D. & Macdonald, R. L. Enhancement of recombinant alpha 1 beta 1 gamma 2L gamma-aminobutyric acidA receptor whole-cell currents by protein kinase C is mediated through phosphorylation of both beta 1 and gamma 2L subunits. *Molecular pharmacology* **50**, 185–195 (1996).
62. Poisbeau, P., Cheney, M. C., Browning, M. D. & Mody, I. Modulation of synaptic GABAA receptor function by PKA and PKC in adult hippocampal neurons. *The Journal of neuroscience: the official journal of the Society for Neuroscience* **19**, 674–683 (1999).
63. Connolly, C. N., Wooltorton, J. R., Smart, T. G. & Moss, S. J. Subcellular localization of gamma-aminobutyric acid type A receptors is determined by receptor beta subunits. *Proceedings of the National Academy of Sciences of the United States of America* **93**, 9899–9904, <https://doi.org/10.1073/pnas.93.18.9899> (1996).
64. Mhyre, T. R., Maine, D. N. & Holliday, J. Calcium-induced calcium release from intracellular stores is developmentally regulated in primary cultures of cerebellar granule neurons. *Journal of neurobiology* **42**, 134–147 (2000).
65. Alonso, M. T., Chamero, P., Villalobos, C. & Garcia-Sancho, J. Fura-2 antagonises calcium-induced calcium release. *Cell calcium* **33**, 27–35, [https://doi.org/10.1016/s0143-4160\(02\)00179-3](https://doi.org/10.1016/s0143-4160(02)00179-3) (2003).
66. Carter, A. G., Vogt, K. E., Foster, K. A. & Regehr, W. G. Assessing the role of calcium-induced calcium release in short-term presynaptic plasticity at excitatory central synapses. *The Journal of neuroscience: the official journal of the Society for Neuroscience* **22**, 21–28 (2002).
67. Meier, S. D., Kafitz, K. W. & Rose, C. R. Developmental profile and mechanisms of GABA-induced calcium signaling in hippocampal astrocytes. *Glia* **56**, 1127–1137, <https://doi.org/10.1002/glia.20684> (2008).
68. Kang, J., Jiang, L., Goldman, S. A. & Nedergaard, M. Astrocyte-mediated potentiation of inhibitory synaptic transmission. *Nature neuroscience* **1**, 683–692, <https://doi.org/10.1038/3684> (1998).
69. Serrano, A., Haddjeri, N., Lacaillle, J. C. & Robitaille, R. GABAergic network activation of glial cells underlies hippocampal heterosynaptic depression. *The Journal of neuroscience: the official journal of the Society for Neuroscience* **26**, 5370–5382, <https://doi.org/10.1523/JNEUROSCI.5255-05.2006> (2006).
70. De Erasquin, G., Brooker, G., Costa, E. & Wojcik, W. J. Stimulation of high affinity gamma-aminobutyric acidB receptors potentiates the depolarization-induced increase of intraneuronal ionized calcium content in cerebellar granule neurons. *Molecular pharmacology* **42**, 407–414 (1992).
71. Mariotti, L., Losi, G., Sessolo, M., Marcon, I. & Carmignoto, G. The inhibitory neurotransmitter GABA evokes long-lasting Ca(2+) oscillations in cortical astrocytes. *Glia* **64**, 363–373, <https://doi.org/10.1002/glia.22933> (2016).
72. Pierce, K. L., Premont, R. T. & Lefkowitz, R. J. Seven-transmembrane receptors. *Nature reviews. Molecular cell biology* **3**, 639–650, <https://doi.org/10.1038/nrm908> (2002).
73. Zeng, W. *et al.* A new mode of Ca2+ signaling by G protein-coupled receptors: gating of IP3 receptor Ca2+ release channels by Gbetagamma. *Current biology: CB* **13**, 872–876, [https://doi.org/10.1016/s0960-9822\(03\)00330-0](https://doi.org/10.1016/s0960-9822(03)00330-0) (2003).
74. Smrcka, A. V. & Sternweis, P. C. Regulation of purified subtypes of phosphatidylinositol-specific phospholipase C beta by G protein alpha and beta gamma subunits. *The Journal of biological chemistry* **268**, 9667–9674 (1993).
75. Bugrim, A. Regulation of Ca2+ release by cAMP-dependent protein kinase A mechanism for agonist-specific calcium signaling? *Cell calcium* **25**, 219–226 (1999).
76. Eccles, J. C., Ito, M. & Szentágothai, J. The Cerebellum as a Neuronal Machine (1967).
77. Berglund, K., Wen, L., Dunbar, R. L., Feng, G. & Augustine, G. J. Optogenetic Visualization of Presynaptic Tonic Inhibition of Cerebellar Parallel Fibers. *The Journal of neuroscience: the official journal of the Society for Neuroscience* **36**, 5709–5723, <https://doi.org/10.1523/JNEUROSCI.4366-15.2016> (2016).
78. Silver, R. A., Colquhoun, D., Cull-Candy, S. G. & Edmonds, B. Deactivation and desensitization of non-NMDA receptors in patches and the time course of EPSCs in rat cerebellar granule cells. *The Journal of physiology* **493**(Pt 1), 167–173 (1996).
79. Hernandez-Rabaza, V. *et al.* Neuroinflammation increases GABAergic tone and impairs cognitive and motor function in hyperammonemia by increasing GAT-3 membrane expression. Reversal by sulforaphane by promoting M2 polarization of microglia. *Journal of neuroinflammation* **13**, 83, <https://doi.org/10.1186/s12974-016-0549-z> (2016).
80. Kaupmann, K. *et al.* Expression cloning of GABA(B) receptors uncovers similarity to metabotropic glutamate receptors. *Nature* **386**, 239–246, <https://doi.org/10.1038/386239a0> (1997).
81. Courjaret, R., Troger, M. & Deitmer, J. W. Suppression of GABA input by A1 adenosine receptor activation in rat cerebellar granule cells. *Neuroscience* **162**, 946–958, <https://doi.org/10.1016/j.neuroscience.2009.05.045> (2009).
82. Sachidanandan, D., Reddy, H. P., Mani, A., Hyde, G. J. & Bera, A. K. The Neuropeptide Orexin-A Inhibits the GABAA Receptor by PKC and Ca(2+)/CaMKII-Dependent Phosphorylation of Its beta1 Subunit. *Journal of molecular neuroscience: MN* **61**, 459–467, <https://doi.org/10.1007/s12031-017-0886-0> (2017).
83. Chavis, P., Shinozaki, H., Bockaert, J. & Fagni, L. The metabotropic glutamate receptor types 2/3 inhibit L-type calcium channels via a pertussis toxin-sensitive G-protein in cultured cerebellar granule cells. *The Journal of neuroscience: the official journal of the Society for Neuroscience* **14**, 7067–7076 (1994).
84. Thompson, M. D., Xhaard, H., Sakurai, T., Rainero, I. & Kukkonen, J. P. OX1 and OX2 orexin/hypocretin receptor pharmacogenetics. *Frontiers in neuroscience* **8**, 57, <https://doi.org/10.3389/fnins.2014.00057> (2014).
85. Rothman, J. S. & Silver, R. A. NeuroMatic: An Integrated Open-Source Software Toolkit for Acquisition, Analysis and Simulation of Electrophysiological Data. *Frontiers in neuroinformatics* **12**, 14, <https://doi.org/10.3389/fninf.2018.00014> (2018).
86. Sigworth, F. J. The variance of sodium current fluctuations at the node of Ranvier. *The Journal of physiology* **307**, 97–129, <https://doi.org/10.1113/jphysiol.1980.sp013426> (1980).
87. Hines, M. L. & Carnevale, N. T. The NEURON simulation environment. *Neural computation* **9**, 1179–1209 (1997).
88. Diwakar, S., Magistretti, J., Goldfarb, M., Naldi, G. & D'Angelo, E. Axonal Na+ channels ensure fast spike activation and back-propagation in cerebellar granule cells. *Journal of neurophysiology* **101**, 519–532, <https://doi.org/10.1152/jn.90382.2008> (2009).
89. McDougal, R. A. *et al.* Twenty years of ModelDB and beyond: building essential modeling tools for the future of neuroscience. *Journal of computational neuroscience* **42**, 1–10, <https://doi.org/10.1007/s10827-016-0623-7> (2017).

## Acknowledgements

We are grateful to members of the Pugh lab for helpful discussion and comments on data collection and analysis. We would particularly like to thank Rebecca Howell for her contributions to this work. This work was funded by National Institutes of Health, Grant # R01 NS092809.

## Author contributions

S.N.K., W.C.W. and Y.Y. collected and analyzed data. S.N.K. and J.R.P. designed experiments and interpreted the data. S.N.K. created the figures and wrote the first draft of the manuscript. J.R.P. edited the final draft of the manuscript.

## Competing interests

The authors declare no competing interests.

### Additional information

**Correspondence** and requests for materials should be addressed to J.R.P.

**Reprints and permissions information** is available at [www.nature.com/reprints](http://www.nature.com/reprints).

**Publisher's note** Springer Nature remains neutral with regard to jurisdictional claims in published maps and institutional affiliations.



**Open Access** This article is licensed under a Creative Commons Attribution 4.0 International License, which permits use, sharing, adaptation, distribution and reproduction in any medium or format, as long as you give appropriate credit to the original author(s) and the source, provide a link to the Creative Commons license, and indicate if changes were made. The images or other third party material in this article are included in the article's Creative Commons license, unless indicated otherwise in a credit line to the material. If material is not included in the article's Creative Commons license and your intended use is not permitted by statutory regulation or exceeds the permitted use, you will need to obtain permission directly from the copyright holder. To view a copy of this license, visit <http://creativecommons.org/licenses/by/4.0/>.

© The Author(s) 2019